EUROPEAN SPALLATION SOURCE

Estia - Preliminary System Design

Version 1.8

	Name	Affiliation
Authors	Artur Glavic, Sven Schütz	PSI
Reviewers	Jorgen Andersson	ESS
	Phil Bentley	ESS
	Thomas Gahl	ESS
	Francesco Piscitelli	ESS
	Hanna Wacklin	ESS
TG2 Review Committee	Shane Kennedy (Chair)	ESS
	Ken Andersen	ESS
	John Ankner	STAP
	Robert Cubitt	STAP
	Sylvain Désert	LLB
	Richard Hall-Wilton	ESS
	Arno Hiess	ESS
	Gábor László	ESS
	Iain Sutton	ESS
Approver	Andreas Shreyer	ESS

February 2, 2017

European Spallation Source ESS AB
Visiting address: ESS, Tunavägen 24
P.O. Box 176
SE-221 00 Lund
SWEDEN
www.esss.se

Contents

1. Introduction

1.1. Purpose of the document

The Preliminary System Design Description of the *Estia* instrument describes the system architecture and the physical layout of the instrument. The hardware and software descriptions result from the design work based on the functional requirements (1) as well as the constraint requirements that have been identified at this point. The purpose of this document, together with the System Requirements and Concept of Operations documents is to:

- Provide a documented description of the design of the instrument that can be reviewed and approved by the stakeholders in a Tollgate review
- Provide a description of the instrument in enough detail that its component parts can be designed in detail ("design-to specification")
- Provide a description of the hardware and software system components in sufficient detail to assess whether they fulfil the functional requirements
- Discuss the expected scientific performance of the instrument

1.2. Definitions, acronyms and abbreviations

Abbreviation	**Explanation of abbreviation**
PBS	Product breakdown structure
BTCS	Beam transport and conditioning system
SES	Sample exposure system
SCS	Scattering characterization system
NOSG	ESS neutron optics and shielding group
PNR	Polarized Neutron Reflectometry
VS	Virtual Source

Specific to neutron guides:	
Abbreviation	**Explanation of abbreviation**
segment	A single physical piece of a neutron guide as produced by the vendor.
mirror	A collection of segments that belong to the same geometrical shape or serve the same physical purpose. An example would be an elliptical mirror, which describes one reflector with elliptic shape that is implemented using several segments.
guide	One or more mirrors that share the same location on the beam axis and form one component of the beam delivery system. An example would be an elliptical guide that is a collection of four elliptical mirrors, two opposite mirrors for horizontal and vertical direction, each.
guide system	The collection of neutron guides that form the full beam delivery system from source to sample.

2. System Characteristics

2.1. System purpose

The *Estia* instrument is a vertical sample reflectometer with polarization analysis optimized for small, solid samples. To allow the measurement of down to $\leq 1\,\mathrm{mm}^2$ sample surface with sufficient intensity it is based on the focusing reflectometry[1] principle using a *Selene* neutron guide[2]. *Estia* will primarily serve the hard condensed matter community as complimentary instrument to the horizontal sample reflectometer $FREIA$, providing a larger q-range and sample environment for diverse magnetic experiments to ESS.

2.2. System overview

The instrument consists of three main technical subsystems: the beam transport and conditioning system (BTS), the sample exposure system (SES) and the scattering characterisation system (SCS). In addition, as described in the instrument product breakdown structure (PBS), the instrument includes the structures that house and support these subsystems, the software to control the instrument and the software to process the data. The hardware description in this document does not strictly follow the PBS, but rather a functional breakdown of technical components along the neutron beam path. This makes it easier to map the specifications to the high level scientific requirements. PBS numbers are given for reference where appropriate.

All components listed within this document are part of the initial scope funded by the NSS construction project. Additional upgrades are explained in the Initial Operations and Staging Plan document.

3. Instrument Overview (13.6.9)

A full overview of the *Estia* instrument is shown in Figure 3.1. There are four main areas starting from the source; inside the bunker (1), between bunker and experimental cave (2), the experimental cave (3) and the instrument control hutch (4).

The main components within the bunker are the neutron feeder (5 - Sec. 4.1) and the chopper pit (6), which houses heavy collimation, the chopper (Sec. 4.3) and the Virtual Source (Sec. 4.4.1). The instrument vacuum system (Sec. 4.6) begins at the position of the gamma shutter.

Starting within the bunker wall is the first of two Selene guide mirrors (7), which are the main component for the beam delivery system (Sec. 4.2). Between the two guides (8) is the instrument shutter (Sec. 4.7.4), middle focus (Sec. 4.4.2), housing some apertures and attenuators, and the neutron polarizer (Sec. 4.5.1).

The experimental cave houses the in-cave optics (9 - Sec. 4.4.3), the sample exposure system (10 - Sec. 5) and the beam characterization system (11 - Sec. 6) with detector and polarization analyzers. Sample preparation equipment (Sec. 9.1) can be found at the cave entrance (12).

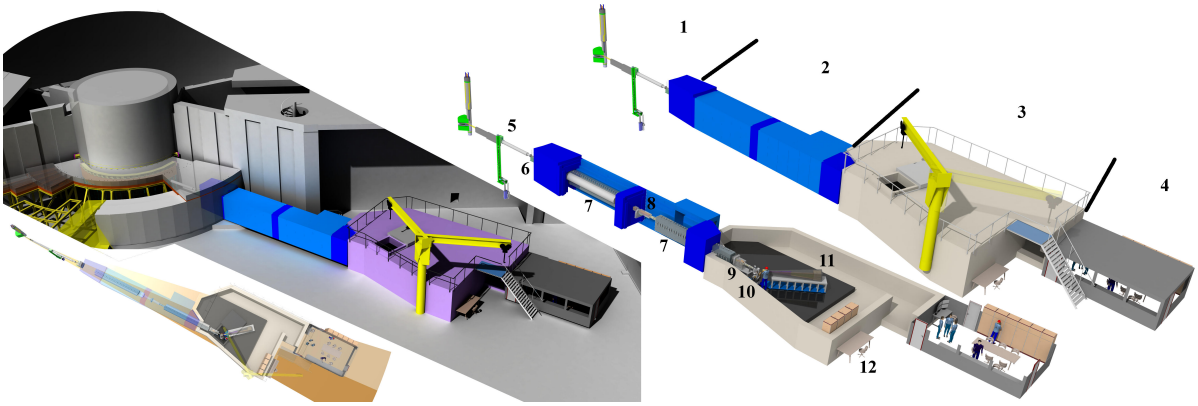

Figure 3.1.: *Estia* overview: Top view showing the 6° wedges of E02 and E01 (left); instrument within the east hall (2^{nd} from left); perspective view with opened (2^{nd} from right); and closed shielding/roof (right).

3.1. Table of component positions

The following table summarizes the geometrical parameters ans positions of the most important components of *Estia*. The distance is defined from the first focal point of the feeder (origin) in the direction of the common c-axes (source-sample line). For the TCS equivalent see 4.1. Defining geometrical parameters are derived as most natural values for the individual component geometry, e.g. width x height x length for a cuboid shape or the short half axis (b) and half focus distance (c) for ellipses.

Item	Category	Defining parameters (e.g. WxHxL) [mm]	Start from origin [mm]	End from origin [mm]
Inner Feeder	Elliptic Guide	focus1=0;b=96;c=5500;m=4	2200	5355
Heavy Collimator 1 (Cu-wedge)	Shielding	L=3000;insert envelope	2300	5300
Monolith Al Window	Vacuum Window	thickness=27	5358	5385
Gamma Shutter	Shutter	D=422	5387	5809
Instrument Entrance Al Window	Vacuum Window	thickness=1	5385	5386
Outer Feeder	Elliptic Guide	focus1=0;b=86;c=5500;m=4	5600	9177
Heavy Collimator 2 (FeNi-collor)	Shielding	WxHxL=180x180x580	10200	10780
BW Chopper	Disk Chopper	D=700; opening=100°	10833	
Virtual Source	Slit	max WxH=10x15; min WxH=0x0	11000	
Heavy Collimator 3 (W+ -collor)	Shielding	r=80;L=300	11288	11588
Heavy Collimator 4 (Cu+ -collor)	Shielding	WxHxL=500x500x1000	12197	13197
Selene 1	Elliptic Guide	b=104.7;c=6000;m=4	13400	20600
Heavy Collimator 5 (Cu+-T-wedge)	Shielding	WxHxL=(400)x500x1600	16200	17800
Instrument Shutter 1 (^{6}Li)	Shutter	fast/fail-safe	20850	
Heavy Collimator 6 (Cu+ C-wedge)	Shielding	WxHxL=457x500x1000	20875	21605
Instrument Shutter 2 (Pb T)	Shutter	slow/fill HC6 gap	21405	21605
Polarizer/Frame-Overlap 1	Spiral Mirror	α=1.65°;m_{pol}=5.0	21742	22759
Middle Focus Components	Item Changer	rotary absorber/mask changer	23000	
Polarizer/Frame-Overlap 2	Spiral Mirror	α=1.65°;m_{pol}=5.0	23241	24258
Selene 2	Elliptic Guide	b=104.7;c=6000;m=4	25200	32400
Slit System	Slit	max WxH=70x160; min WxH=0x0	32985	
RF Spin-Flipper 1	Flipper		33447	33727
Saphire Exit Window	Vacuum Window		34906	
Sample Position	Sample		35000	
RF Spin-Flipper 2	Flipper		35339	35619
Double Analyzer	Spiral Mirror	α=1.4/1.6;m_{pol}=5.0/4.0	35588	37632
Detector Position	Detector		39000	
Beamstop (B_4C equivalent+Fe)	Absorber	WxH=250x600	42500	43000

4. Beam Transport and Conditioning System (13.6.9.1)

The neutron optical system consists of the beam extraction system (PBS 13.6.9.1.1), beam delivery system (PBS 13.6.9.1.2), beam geometry conditioning (PBS 13.6.9.1.4) and beam filtering system (PBS 13.6.9.1.5). Their common purpose is to transport the neutron beam with reflective elements from the moderator to the sample exposure system (PBS 13.6.9.2).

4.1. Neutron Feeder (Beam Extraction System 13.6.9.1.1))

The beam extraction system is oriented to the top-moderator at the following TCS coordinates (beamline origin):

X	116.965
Y	-89.71
Z	137
Y_{rot}	-0.7°
Z_{rot}	-29.5°

The initial beam extraction system, referred to as the feeder, is a neutron guide consisting of planar-elliptical mirrors on three sides (top,bottom,right looking down-stream) where each neutron trajectory undergoes exactly two reflections (top+right or bottom+right). The feeder is oriented towards the top-moderator and needs to transport an initial surface area of 300 mm^2 (10 mm ·30 mm). The focus to focus distance is 11 m, it starts 2.2 m away from the moderator-focus point (beamline origin) and ends at 9.2 m.

Due to the crossing of the monolith-wall it is divided into an internal part which is mounted within the insert and an external part which starts at the monolith vacuum-window. In contrast to the ESS default solution the guide outside the monolith window is not continued within the shutter mechanics, as the accuracy of the kinematic mounts would not be sufficient to fulfill the angular accuracy required. The feeder therefore continues down-stream of the shutter and to avoid gaps in the divergence the inner elliptic guide will be larger as proposed in the optics manual *ESS-0039408*. Simulations

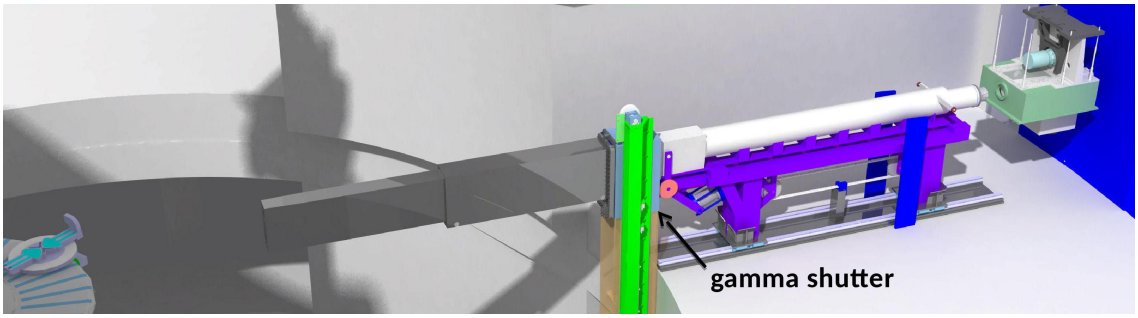

Figure 4.1.: Feeder with a gap at the position of the gamma shutter.

performed with McStas confirm that the small 600 mm gap has no negative impact on intensity or phase space homogeneity for samples below 10x10 mm^2. The outer feeder is housed within a vacuum chamber mounted on a stable frame with kinematic adjustmable mounts. The guide curvature together with in-feeder heavy collimation ensures that the Virtual Source (Sec. 4.4.1) and with that the bunker feed through is out of line of sight from the moderator.

The guide is build of 4-sided metal segments with up to 1.5 m length and m=4 Ni/Ti supermirror coating (**13.6.9.1r1**). Each segment is kept and aligned with a kinematic bearing with position-accuracy sufficient to stay within the highest angular accuracy requirements (**13.6.9.1r6**). The motion and interfacing of the outer feeder segments will be designed to not compromise these requirements.

Although the second beam path is not within the initial construction scope the moderate cost of a double feeder will be payed to avoid the much increased upgrade costs after these components have been activated. Therefore the feeder will already accommodate both beam paths.

4.2. Beam Delivery System

The beam delivery after the Virtual Source (Sec. 4.4.1) will be performed based on the *Selene* guide concept [1] for two separate vertical beam paths that cross at each focal point. Although only one of these paths will be initially installed the feeder and other system components will already be designed to allow the full two beam operation after guide upgrade.

The the divergent beam from the Virtual Source will be refocused with reflections on two perpendicular planar-elliptical mirrors as shown in figure 4.2. The compensation of aberration will be accomplished by a second identical set of mirrors, which are placed on the same guide-axis (long half axis of the ellipses).

The full guide-system can be divided into 3 guides as shown in figure 4.3. The *Guide 1/Feeder*, described in the previous section, will lead from the moderator to the virtual

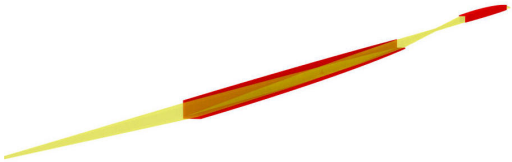

Figure 4.2.: Selene concept

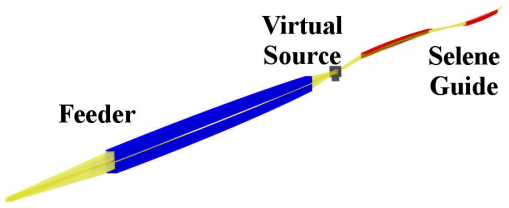

Figure 4.3.: System with double feeder

source and does not have to be truly focusing since the footprint for the sample is generated at the virtual source and much smaller than the moderator. *Guide 2/Selene 1* will refocus the beam to the middle focus and will need to be aligned with a higher precision. The second high precision mirror is *Guide 3/Selene 2* which will focus the beam to the sample, correcting coma aberration for a correct image of th Virtual Source onto the sample.

4.2.1. *Selene* Neutron Guide (Beam Delivery System 13.6.9.1.2))

Each *Selene* guide will consist of a 7.5 m long granite-carrier, which will be designed to assure high structural stability over time. The carriers will be mounted with three kinematic mounting posts onto a motorized hight adjustment (see Fig. 4.4a). Due to the size of the guides a thermal stabilization with a tolerance of 0.1K will be required, which can be achieved by placing the whole granite-carriers into a vacuum chamber and connecting a water bath thermostat to the kinematic mounting points. The vacuum housing together with the kinematic posts will be placed on the foundation with manual adjustment for hight and both horizontal degrees of freedom (**13.6.9.1r8-13.6.9.1r11**).

The adjusters for the mirror segments will consist of motorized actuators fixed to the inner granite surface to minimize effects of thermal expansion. Each actuator element will consist of a stepper motor, a gear box, a connection rod with length compensation, a self holding fine adjustment screw and appropriate couplings. Neutron supermirrors with m=4 (**13.6.9.1r2**) will be attached to the adjusters with kinematic mounting points similar to those shown in Figure 4.4b. Exchanging individual segment pairs (one vertical plus one horizontal reflector) from the front is easily possible, as the optics are self holding by their own weight with only on set of springs on the front surface of the top and bottom segments. The combination of these precise adjustments with the stability of the granite carrier and the thermal stabilization will achieve the necessary accuracy of 1.5 μm over 500 mm segments (**13.6.9.1r7**).

Positioning metrology for the guides will be possible with 3 separate methods. The guide carriers can be placed within the ESS metrology grid during maintenance cycles by using the standard reflectors on precise mounting points on the top of the carrier and the holder frame. In addition hydrostatic monitors above each of the kinematic posts will allow on-line readjustment of the vertical position as proposed in *ESS-0039408*. For the

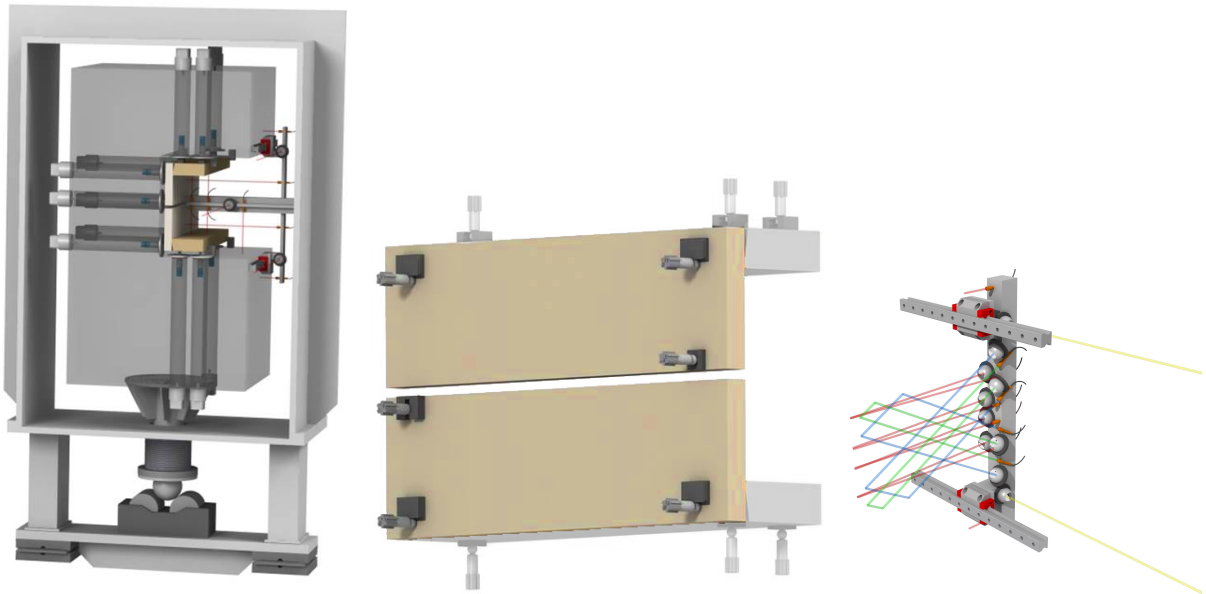

(a) Carrier in vacuum housing (b) Attachment of segments to adjusters (c) Metrology cart

Figure 4.4.: *Selene* guide concept

high accuracy relative positioning of the segments in each *Selene* guide, a fixed metrology cart (Fig. 4.4c) will be attached to the granite block. The cart will have several fiber coupled collimators and retroreflectors that can be used to reflect a laser from the mirror segments to the reflector and back. Each of these collimators will be connected to a central absolute distance interferometer device (*Etalon Multiline*^{TM}), allowing the measurement of the mirror surface distance to the cart with sub-μm precision. Finally, the cart position with respect to a given plane parallel to the elliptical axes will be measured by two additional interferometer heads pointing towards a precise surface of the granite carrier and separately by camera sensors measuring the position of two single mode laser beams shining parallel to the same surface.

4.3. Chopper (13.6.9.1.3)

The copper will be positioned between the shielding and the virtual source at ≈10.84 m from the source and run at 14 Hz (**13.6.9.1r12**). At this position with a detector distance of 39.0 m and avoiding frame overlap with a 2.4 ms gap between pulses the chopper opening is 100.06°. The smallest frame overlap wavelength is 30.07Å, which is filtered with the polarizer or frame overlap mirror. With this geometry the chopper can also be operated in pulse skipping mode, allowing frame overlap free operation in 1/2 and even 1/3 source frequency (expanding the 7Å band (**13.6.9.1r14**) to 14Å and 21Å, respectively). Figure 4.5 shows a sketch of the chopper and detector relation in time of

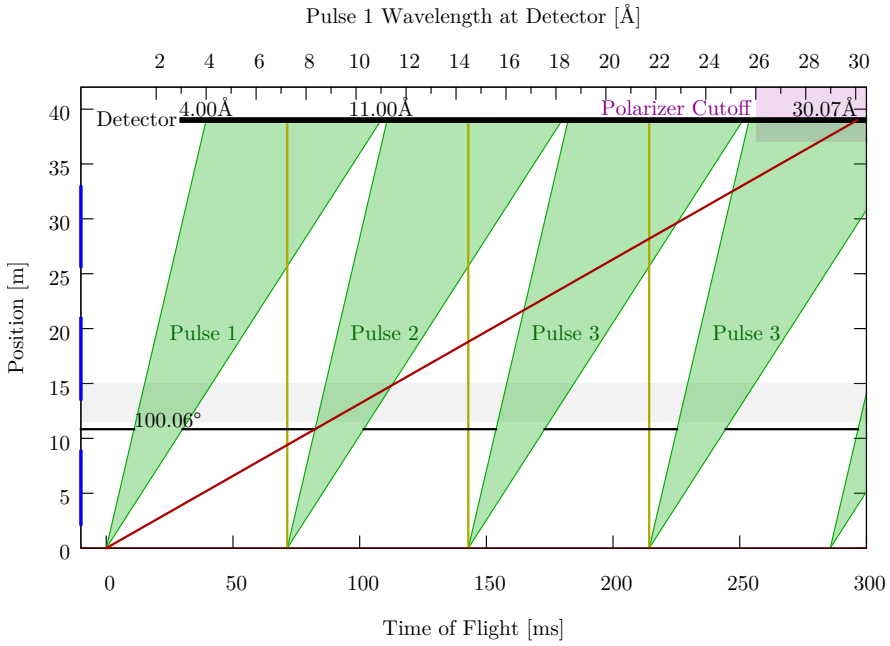

Figure 4.5.: Time-Distance diagram for the selected chopper configuration.

flight. If the large opening angle can't be achieved with the standard chopper system described below an alternative 7 Hz operation with two 50.03° slots can be used.

Choppers based on a standard design with 700 mm diameter disc, as available from *Mirotron*, will be used to keep costs low, as no extraordinary requirements have to be met. The total width of the assembly will be ≤900 mm. With this disc size and close to the virtual source the opening/closing time is below 1 ms, even for a fully opened virtual source aperture (**13.6.9.1r13**). A drawing and example image of such a chopper assembly is shown in figure 4.6.

The bottom of the housing will be modified to connect with a connection plate, following the ESS CHIM specifications, to a vacuum vessel common with the other optical components. Four standard pillars as defined in *ESS-0039747* will be used to guide the chopper assembly during mounting, minimizing the risk of damage to the assembly and surrounding equipment. A top plate (*ESS-0033150* specification) will be attached to the assembly. This will allow direct access for maintenance from the top without personal presence within the bunker shielding boundaries. Currently the extractable assembly is expected to have a mass of 200kg (<2T). The whole chopper pit will be founded on the instrument base plate separately from other components and the vacuum vessel will use standard 160CF flanges and bellows following the ESS specification to achieve proper mechanical decoupling. The mounting bolts (*ESS-0041943* compliant), plate and pit structure will be sufficiently strong to achieve structural integrity in the case of catastrophic rotor failure and a 0.4g vertical seismic event. Leveling will be done using four rods cast into the base plate using grout. The alignment and leveling range will exceed ±5 mm with an alignment precision of 0.1 mm using M20x1.5 screws for compatibility.

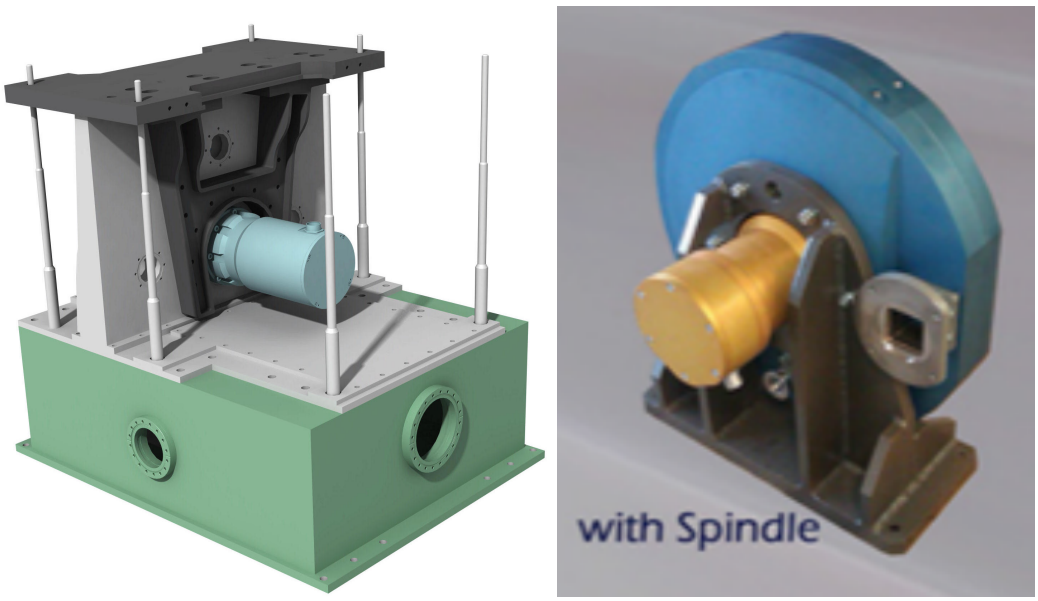

Figure 4.6.: Chopper as implemented in preliminary design with vacuum and CHIM interface (left) and photo of example variant from Mirotron (right).

The shape of the vacuum vessel will allow the placement of the virtual source and a heavy collimator up to 1 cm close to the chopper disk. There will be a bellowed opening at the bottom of the vessel for mounting of the virtual source to enable a separate foundation to prevent vibration.

The chopper motor will point up-stream in the direction of the source to allow enough vertical space for the virtual source. A standard connector plate as defined in *ESS-0041173* will be mounted at the down-stream side of the chopper assembly vessel. Within the plate will be three electrical connectors, one utilities connector and provision for an upgrade connection plate. The chopper control will be connected to the chopper control rack outside the bunker via a pit head box as specified in *ESS-0041175*. As a standard chopper assembly will be used the integration with the CHIC system as described in *ESS-0042906* will generally be simple and full compliance with the specifications is expected.

The materials used will comply with *ESS-0042895* and only components as described in *ESS-0034258* will be incorporated.

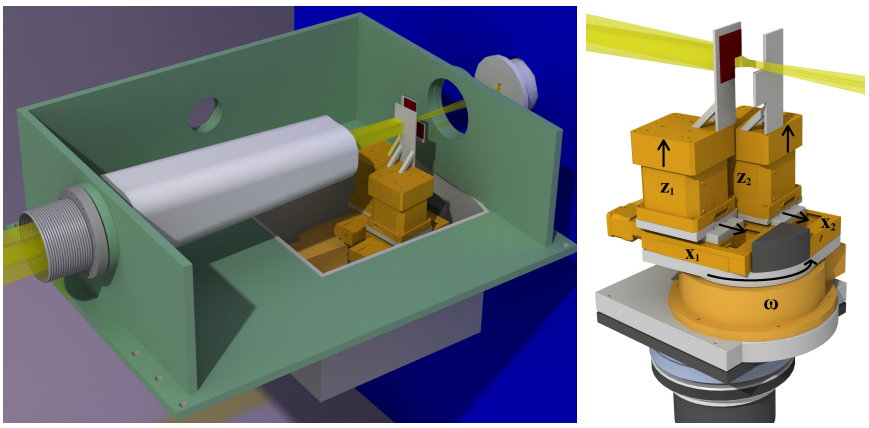

Figure 4.7.: Virtual Source stage, within the chopper pit vacuum box (left) and stand alone (right) illustrating the different positioning stages.

4.4. Beam Geometry Conditioning (13.6.9.1.4)

4.4.1. Virtual Source (Aperture Collimation System)

Directly downstream of the chopper disk, within the same vacuum box, resides a set of neutron absorber blades, which define the beam shape at the first focal point of the Selene guide system. As this new shape is imaged by the focusing optics onto the sample position without much influence of the cold neutron source geometry it is called a Virtual Source (VS). The typical shape of the beam on the sample is several mm tall but only some 10 mm wide, which needs to be supplied by the VS. The absorbers are L-shaped blades with a frame to fix them on standard translation stages. Directly below the frames precision z-translation stages, which in turn are attached to horizontal translation stages. With these four stages the opening height and absorber distance (in beam direction) can be controlled while keeping the vertical edges parallel. All these components together with a proper counter weight are mounted on a vertical axis rotation stage, which can follow the sample ω-angle to keep the VS as large as the sample footprint. The VS assembly is shown in Figure 4.7 within the chopper pit vacuum box and with a separate view form another angle.

The rotation stage itself is fixed on a kinematic mounting plate, that can be pulled up from the top after the chopper has been removed and allows precise repositioning after maintenance. Electronic connections from the motors will be bundled to a connector at the top of the plate, which will be linked to an out-of-vacuum connector accessible from top, as well. Foundation for the kinematic mounting plate is connected to a separate base plate through the bottom of the vacuum box using a bellowed flange. This allows the complete mechanical decoupling of the sensitive VS components from the chopper assembly.

The advantages of using this stacked stages with L-shaped absorbers over a conventional

slit system are the high accuracy in keeping the absorber blades parallel (**13.6.9.1r22**) and the far separation of the motors to the absorbers and the main beam. As the VS is within the bunker area and close to the open direct beam, a large radiation field can be expected limiting the usability of precise positioning equipment.

With the large separation between absorbers and the first stage (which can even be increased, as the absorbers are very light weight and can be extended when moving away the z-stages downward) the radiation dose at the motor positions will be largely reduced and by placing suitable absorber material like lead between the blades and stages one can expect reductions of the radiation dose at sensitive components by a factor of 10 or more.

Figure 4.8.: Middle focus changer

4.4.2. Middle focus aperture system

For alignment and beam characterization purposes it can be useful to separate the contributions of the first and the second Selen guide. For this task a set of horizontal and vertical slits as well as pin-holes will be installed at the position of the focus between the two ellipses. In addition, a larger rectangular absorber installed during normal operation will allow suppression of neutrons not passing through the focus to prevent parasitic beam paths.

Changing between different apertures will be done with a rotating holder (see Fig. 4.8) mounted on a motorized XZ-stage for precise alignment to the focus position. The middle focus assembly will have an additional hydrostatic monitor to measure the relative alignment to the two Selene guide granite pieces.

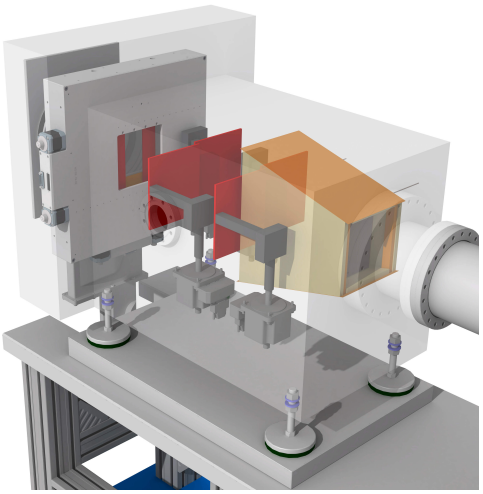

Figure 4.9.: In-cave optics

4.4.3. In-cave optics

After the exit of the second Selene guide, separated from the rest of the beamline by a vacuum valve, will be a box for in-vacuum optical components. The assembly is showin in Figure 4.9.

Beam shaping slit system The beam divergence that reaches the sample can be controlled with a set of horizontal and vertical slits after the end of the second Selene guide. The maximum opening needs to be sufficient to cover the full 4° vertical and 1.5° horizontal divergence but otherwise constitute standard neutron slits. The assembly will either be based on an existing design that has been proven at one of the major neutron facilities or bought as a whole from a commercial supplier to keep costs within reasonable bounds.

4.5. Beam Filtering System (13.6.9.1.5)

4.5.1. Neutron Polarisation System

Two double-side coated transmission polarizing supermirrors will be installed before and after the middle focus (see Fig. 4.10). The mirrors will be placed vertically with the shape of logarithmic spirals to keep a constant incident angle of ≈1.65° for all neutrons passing through the middle focus. The coating will be Fe/Si with m=5 to achieve a good polarization even for neutrons passing through it under slightly different angles. With this configuration the refraction offset from the first mirror will be corrected in first order by the second mirror.

Figure 4.10.: Polarizing mirrors and frame overlap mirrors before and after middle focus

The mirrors will be mounted in a strong guide field within a frame on a translation stage that allows to position it perpendicular to the beam and move it out of the beam path entirely.

Polarization efficiency and transmission expected for this configuration is $P > 99.5\%/T > 44\%$ for 4Å neutrons and $P > 99.9\%/T > 30\%$ for 11Å neutrons. The natural critical edge of Si at m≈0.65 leads to total reflection of all neutron wavelength larger than 28Å. This will be used to suppress long wavelength contamination within the beam from the second frame passing the chopper, which starts at 30Å.

4.5.2. Guide Fields

To keep the neutron spin direction after polarization, it is necessary to have a homogeneous guide field from the middle focus until the sample. This will be done by external iron plates connected with permanent magnets in the areas without neutron guides. Within the *Selene* guide 2 region, the guide field will be incorporated into the adjustment system by using the adjuster frames to hold the necessary iron plates, that again are connected with permanent magnets.

4.5.3. Frame Overlap Mirrors

Uncoated silicon pieces with the same shape as the polarizers will be mounted within the same frame to be used as frame overlap filters for unpolarized measurements. The translation stage will be used to switch between the two operation modes.

4.5.4. Neutron Attenuators

As the intensity of *Estia* will likely exceed the capability of the detectors it will need the option to automatically install attenuators to reduce initial beam intensity. These will probably be strong neutron scatterers and therefore produce a large background if placed within the experimental cave. For this reason the attenuators will be installed in the middle focus aperture changer (see section 4.4.2), where the neutron beam is relatively small and scattered beams can't reach the experimental area.

4.6. Vacuum System (13.6.9.1.9)

The *Estia* instrument will have an instrument vacuum system which will consist of a continuous vacuum from the monolith window to the beginning of the sample environment. The minimization of number and thickness of vacuum windows is essential to reduce intensity losses. Therefore the system will have two vacuum-windows; one facing the monolith and one facing the sample (**13.6.9.1r54**).

The vacuum system will be divided into sectors and equipped with vacuum gate valves, which can be closed when the beam is of (**13.6.9.1r53**). Thus the separation, as shown in Figure 4.11, the maintenance of the sections 1, 3, 5 can be performed without breaking the vacuum at the *Selene* guides, as a result the mirror-segment alignment will not be disturbed in consequence of such tasks. Furthermore vacuum gate valves operate as points of separation for individual prealigned components, allowing separate leakage testing. Each sector will be equipped with a separate pumping station that will allow quick and stable evacuation.

When the gamma shutter has to be closed, the vacuum in section 1 will be broken and the the feeder mirror 4.1 will be translated downstream towards the chopper. A bellow will compensate the shortening of the flight-tube.

Most of the vacuum components will be standard commercial products suitable for high vacuum application. The boxes for the chopper pit, in-cave optics, *Selene* guides and other custom components will be designed with the goal of achieving at least 10^{-3} mbar (**13.6.9.1r52**).

4.7. Shielding (13.6.9.1.10)

The shielding serves two purposes: Firstly it limits the radiation levels outside the instrument to safe levels for personnel access, this is coined biological shielding. Suppresses background from radiation not usable for the experiment (undesired beam neutron paths, fast n and γ radiation). The requirements for the latter are much more stringent. The biological shielding for the neutron guide needs to stop any fast and thermalized neutron radiation as well as the γ emmission produced by neutron absorption to stay below the ESS radiation safety *ESS-0001786*.

The *Estia* shielding can functionally be divided in two classes, both are driven by the requirements for biological radiation-shielding and backgroud suppression shielding. One consists of elements that have a structural as well as a radiation shielding function, those will mainly be precast boronated concrete elements or steel frames combined with boronized hydogenious material elements (e.g. wax). It will be used for the Beamline Shielding (PBS 13.6.6.1.10.3) and the Experimental Cave Shielding (PBS 13.6.6.5.4). The second shielding class will be a heavy collimation shielding and consist of elements which will work as apertures and will not provide a primary structural function. This shielding will be used for the In-Bunker Shielding (PBS 13.6.6.1.10.1) and the Neutron Guide Shielding (PBS 13.6.6.1.10.3). The Shielding implementation will be comply with the NOSG Handbooks *ESS-0039408* and *ESS-0052625*.

The design of the bunker is not finished at the time of this document's writing, thus the shielding thicknesses and materials will be specified by the NOSG at a later stage. Further, the geometry and materials of shielding components specified here will be optimized later based on detailed Monte Carlo simulations.

4.7.1. In-Bunker Shielding

The shieling within the bunker is the most essential part of the heavy collimation to get rid of fast n background before it enters the beamline through the bunker wall. All

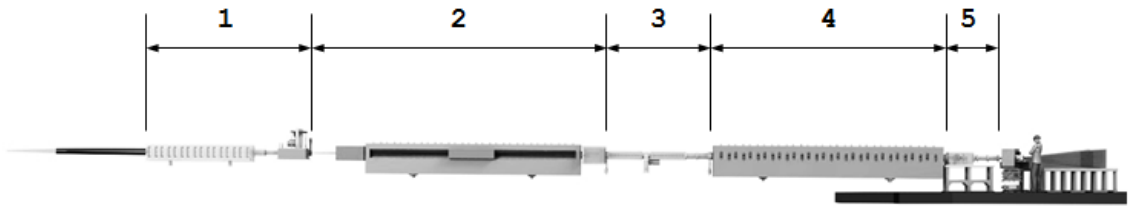

1 feeder section - **2** *Selene* guide 1 section - **3** middle focus section
4 *Selene* guide 2 section - **5** cave section

Figure 4.11.: Vacuum section organisaiton

undesired neutrons that can be scattered away from the main beampath or absorbed at this point significantly reduce the instrument background and, in addition, reduce the radiation leaving the bunker and therefore the need for biological shielding outside the bunker wall.

Insert Shielding

A ≈2 m long piece of copper will be positioned within the monolith insert to block the direct view through the center of the elliptical feeder guide. The shape of the block will follow the beam path both vertically and horizontally as closely as possible within the alignment precision of the insert mechanics. With this shielding block the direct line of sight from the beam extraction point is broken at any point after the end of the feeder mirror.

Collar before chopper

A FeNi collimator of ≈70 cm length and ≈15 cm diameter will be placed directly before the chopper disc and within the chopper pit vacuum box. A central cutout in the shape of the maximum expected usable beam will be present. Precise alignment of the element will be possible with adjustment screws from the top when the chopper has been removed.

This shielding element is close to the point of smallest beam size and will therefore remove a large amount of fast and thermalized neutrons not directy within the usable beam path. In addition it breaks direct line of sight for areas within the monolith further away from the beam extraction point.

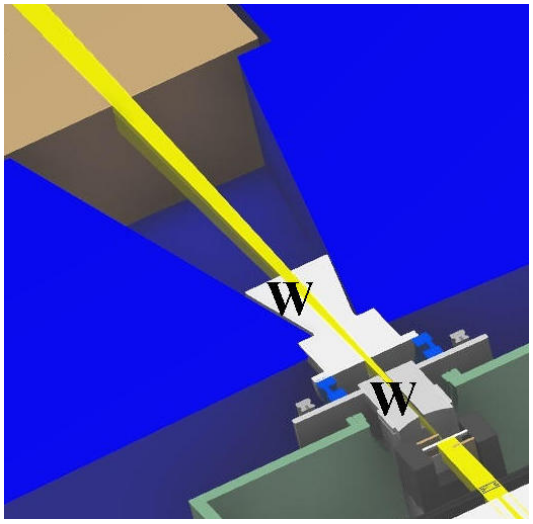

Figure 4.12.: Shielding around VS

Collar after VS

After the VS a combination of 5 cm long W collars (≈1/10th length for fast neutrons) separated by hydogenious B containing elements will be placed reaching into the bunker wall. These blocks will be incorporated into vacuum housings that can be adjusted with respect to the bunker wall. The approximate shape of the combined system is shown in Figure 4.12.

This geometry allows a fast neutron shielding very close to the main beam, independent from the precision of the opening in the bunker wall but with a strong scattering

power and avoiding direct streaming paths between vacuum housing and bunker wall. The height can be readjusted after placing the bunker wall elements to make sure it is positioned correctly for the beam to pass through. With this essential part of the heavy collimation most of the fast neutrons that pass through the first collar by Albedo transport or scattered into the beamline by in-bunker components of neighboring beamlines can be hindered from entering the bunker wall.

4.7.2. Bunker wall

After the W collars, the space within the bunker wall opens up to form a void region for expension of fast neutron cones (*ESS-0039408*). Although this leads to a relatively large whole through the bunker wall, it is expected that the larger scattering power of the FeNi and W collars as well as the first beamline shielding component will overcompensate this missing material for biological shielding.

4.7.3. Beamline Shielding

The main biological beamline shielding will likely consist of liftable elements of a form of concrete, that will have geometrical features to only allow the installation in a certain order (starting from the bunker wall until the cave structure). Joints between separate elements will have chicanes following the 10x rule (*ESS-0039408*) to prevent streaming paths for fast neutron radiation. Specially shaped allements will be installed afer placing all shielding elements for one sector, called keystones, that will lock the other elements in place and can be used for interlock purposes as advised by the ESS PSS group.

To increase the maintenance flexibility and allow limited access to *Selene* guide 2, the structural shielding of the guide system will be divided in two sectors (figure 4.13). The *Selene* guide 1 sector (light-green) with the sector-wall (darkgreen) will form a closed cave with the instrument shutter right before the sector-wall. The *Selene* guide 2 sector (blue) will have a separate keystone, thus access to this section can be granted when the instrument shutter is closed. There will be a separate door to access this area without opening the shielding.

Experimental Cave Shielding

The experimental cave shielding will consist of steal walls, which will be filled with borated parafine, combining structural integrity and shielding both from radiation within the cave and background from neigboring instrument or skyshine.

A beamstop with rough neutron absorbing surface will be placed on the wall opposite to the neutron guide.

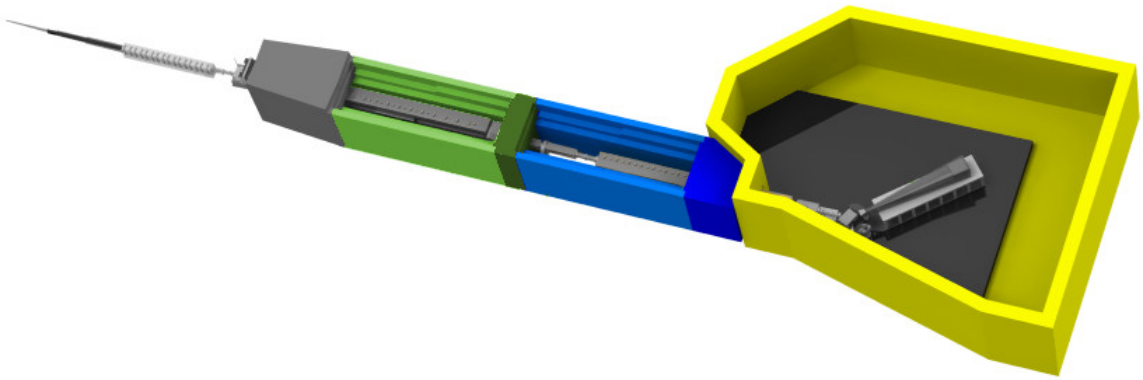

Figure 4.13.: Beamline Shielding Concept.

4.7.4. Neutron Guide Shielding (Heavy Collimation)

The in-bunker shielding components are the first line of defence agains fast neutron background, already reducing this contribution drastically and preventing any direct line of sight from the monolith and indirect line of sight besides the main beam path. Indirect line of sight fast neutrons passing through the collimators parallel to the main beam, however, can reach the first *Selene* guide unhindered.

The neutron guide shielding within the *Selene* 1 area will suppress this background, leading the main beam out of the second line of sight.

Selene Guide 1 Shielding

The heavy collimation for the *Selene* guide 1 will eliminate the direct line of sight (LOS) between middle focus and virtual source. The aim of the section collimation is to purge background and the biological hazard of thermal and cold neutrons, as well as gamma radiation. Therefore a first collimator will be mounted before the guide consisting of copper and borated hydogenious material.

A second collimator of the same materials will be placed in the middle of the guide, where the beams are the furthest away from the direct line and vertically separated so background between the beams can be filtered out as well. This block is similar in geometry and fuction as the insert shielding block.

A third collimator will be placed right before the sector wall after the elliptical guide. Latter will be realized as an aperture and used as part of the instrument shutter, therefore it will be designed to block γ-radiation to enable access to the *Selene* guide 2 seciton and the experimental cave during neutron production. In addition to the collimator block the instrument shutter will consist out of a ^{6}Li thermal neutron absorber, to block

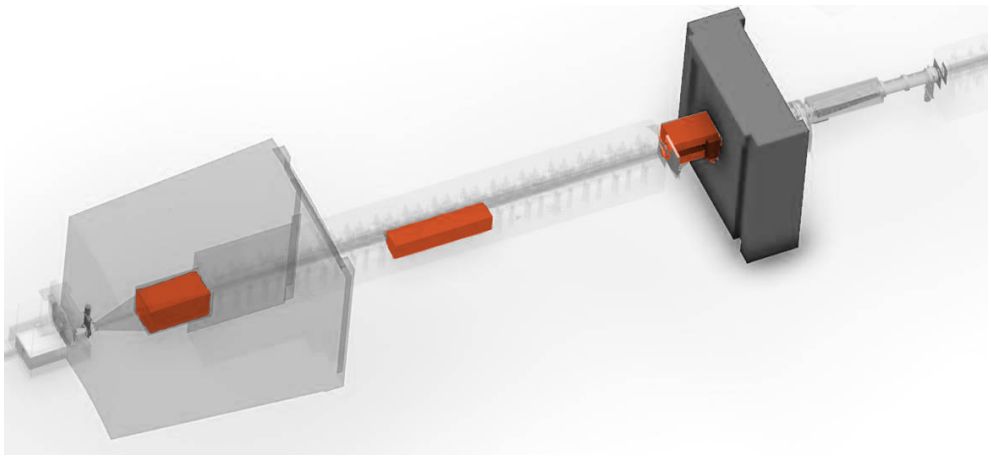

Figure 4.14.: *Selene* Guide 1 Shielding

Figure 4.15.: *Selene* Guide 2 Shielding

the main beam in front of the collimator, and a Pb block that can be moved into the collimator to get rid of any residual γ radiation produced further up-stream. Behind the instrument shutter a radiation sensor will be placed and linked to the PSS-system.

In order to minimize the gap between the heavy collimators and the beam, the collimators will be placed on manually adjustable bearings and realigned during maintenance-periods.

4.7.5. Middle Focus Shielding

If shielding simulations suggest that fast neutron and/or γ background will be a substential issue, additional heavy collimation elements (W/Cu) will be installed before and after the middle focus position, where the beam size is smallest.

Selene Guide 2 Shielding

A potential heavy collimation of the *Selene* guide 2 section will follow the same concept as the one in *Selene* guide section 1, if shielding calculations show that additional reduction of the fast neutron background will be needed. It is expected that this will not be necessary and thus only thermalized neutrons need to be absorbed with simple borated aluminum blades. The thin, light blades can be mounted directly into the granite blocks.

5. Sample Exposure System (13.6.9.2)

The sample exposure system is the part of the beamline directly related to positioning the sample within the neutron beam and to control physical properties relevant to the experiment. This equipment is located within the experimental cave near the final focal point of the *Selene* guide 2.

5.1. Sample Positioning System (13.6.9.2.1)

To allow larges flexibility for sample environment equipment as well as high positioning accuracy paired with fast and convenient sample changes, the sample positioning is separated into rotation around the vertical axis (incident angle ω) and positioning of the sample relative to ω to adjust the reflecting surface with respect to the incident beam.

At the bottom of the sample stage a heavy duty goniometer with optical encoder will be mounted on a frame with air-feet, which enables initial positioning of the rotation axis with respect to the neutron beam. This stage will be able to accommodate any ESS pool sample environment equipment of class L and relevant XL class items needed

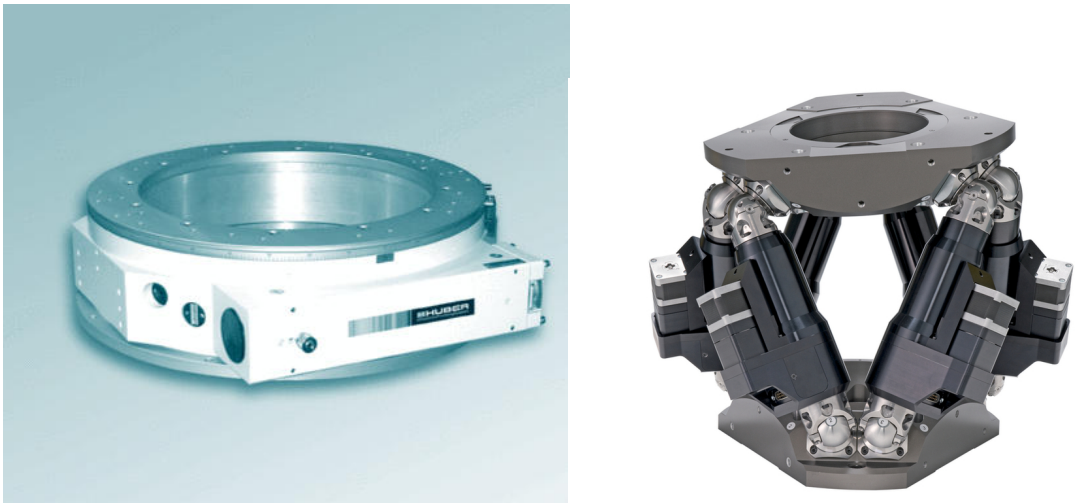

(a) ω Stage Huber 440 (b) Hexapod Newport HXP-1000

Figure 5.1.: Sample positioning equipment

for high magnetic fields, following the guide lines in *ESS-0038078*. For this reason the supported weight will be >800kg (or above if needed for large cryomagnets) using a similar stage as the Huber 440-W1 shown in Figure 5.1a. On top of the rotation stage will be a kinematic mounting plate compatible with the ESS standard (*ESS-0038078*) to allow quick installation of either the *Estia* default SE or pool equipment.

The default instrument specific SE, expected to be used in 80-90% of user experiments, will be placed with a separate frame on the kinematic mount. The frame will house a manually adjustable table holding the magnet and alignment system and a hexapod positioning stage for the cryostat or room temperature sample holder. With a hexapod system similar to the Newport model shown in Figure 5.1b it is possible to adjust all degrees of freedom of the sample with high precision (0.3 μm in the Newport case). In addition, the magnet and laser alignment assembly have a fixed relation to the incident beam, allowing homogeneous magnetic fields at the measured point and fast alignment. This solution will fulfill all relevant system requirements for sample positioning (**13.6.9.2r1**-**13.6.9.2r10**) as well as weight requirements (**13.6.9.2r13**,**13.6.9.2r14**).

The sample holder (or cryostat) is attached to the hexapod with a quick release kinematic mount on a manual linear stage, to allow fast exchange with reproducible placement. This way the sample can be mounted in the cryostat off-line and even cooled down outside the cave before installing it at the instrument.

5.2. Sample Environment Equipment (13.6.9.2.3)

Experience form other sources shows, that reflectometer often need instrument specific sample environment for magnetic fields and low temperatures. The two main reasons being, that reflectometry requires low background from the sample environment, so trying to avoid material within the neutron beam is essential, and that on polarized instruments the number of measurement days with the need for low temperatures and magnetic fields is far above 30%.

5.2.1. Magnetic Fields

Most PNR measurements are performed on ferromagnetic materials, which require only moderate magnetic fields. Therefore flexibility, limited fringe fields and available scattering angle are the main priority when selecting a suitable magnet. Recently, room temperature bore cryomagnet solutions have been developed, that allow relatively large fields without the need for the neutron beam to pass through additional material (**13.6.9.2r22**). Closed cycle coolers further increase the convenient usability of this equipment on a daily basis.

Against the advise of the instrument team it was decided not to include a magnet system into the *Estia* construction budget. Therefore an ESS pool electromagnet will be used

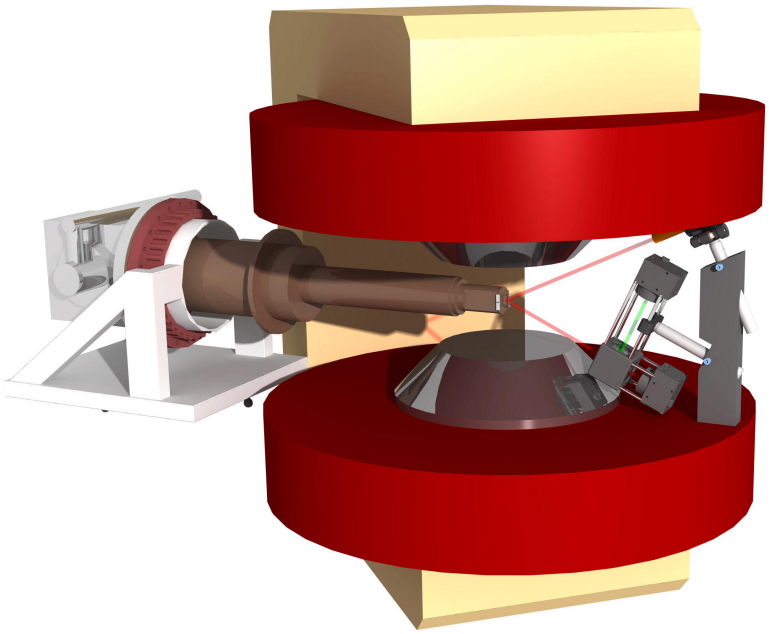

Figure 5.2.: Overview of the sample environment with magnet, cryostat and laser

initially. (It has been agreed with NSS that the pool magnet will be used more than 50% of the time at the *Estia* instrument during that period.) Figure 5.2 shows the expected geometry of such a magnet together with the cryostat and laser alignment setup. With this configuration, the whole accessible angular range of *Estia* will be usable and the quick access to the sample area is ensured.

5.2.2. Sample Holder Plates

All sample stages that will be used at *Estia* will have a standard connection mechanism to install a common sample holder plate (like a dove tail connector). The plates (Fig. 5.3) will have elevated flat surfaces in standard sizes (10x10 mm^2, 5x5 mm^2, etc.) to mount the sample with e.g. vacuum grease. The material will likely be copper for compatibility with a cryostat and several small threads will be present to mount neutron absorbers (B-Al) before, after and above the sample to reduce background.

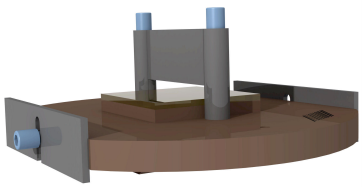

Figure 5.3.: Sample holder

5.2.3. Low Temperatures

Experiment at *Estia* will regularly be performed under low temperature conditions and only need a few minutes to collect full PNR datasets. For this reason the instrument

will use compact liquid He flow cryostats, that can quickly be installed on a kinematic quick release mount. The ESS uses a full helium recovery system, to which the cryostats will be connected.

There are commercially available systems like the one shown in Figure 5.4 from Janis, which are low cost, light weight and allow short cool down times of ≈15 min from 300K to 4K (**13.6.9.2r17**, **13.6.9.2r21**). The achievable base temperature is ≈2K and the cold finger can be equipped with a high temperature option (500K/700K- **13.6.9.2r18**). The vacuum shroud and radiation shield will be customized with windows for the neutron beam (e.g. sapphire) and the alignment laser, if necessary with a IR reflective coating.

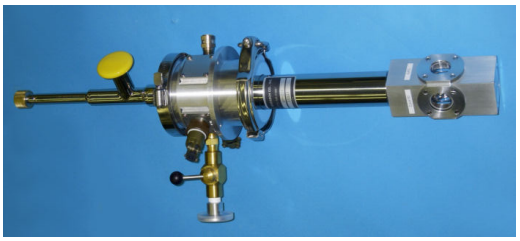

Figure 5.4.: Janis ST LHe cryostat

Electrical connector for transport measurements and electric field application will be present as well as thermal sensors to measure the sample temperature. The cold finger will have the connection mechanism for the sample holder plate described above.

5.2.4. Sample Changer

For room temperature measurements from a large number of samples, a sample changer can be installed with the same kinematic mount used for the cryostat. Figure 5.5 shows a proposed design for such a sample changer that employs the samples with a chain carriage system that is driven by a gear in the back. This solution has the advantage, that it has a small size close to the sample position, can be equipped with a large number of samples (>30), uses cheep standard mechanics commercially available and still allows the adjustment of the sample position with the laser alignment system. The sample holders are attached to the chain at elongated pins present at every 3rd link, have a kinematic alignment points at the back and a sample holder plate connector at the front. At the actual sample position, soft springs at the bottom and top push the holders against a kinematic mount to allow a stable, reproducible sample position during measurements. A switch between two metal pins will be closed when a holder is inserted in it's kinematic mounting points, which will be used as feedback to the motor to define sample positions.

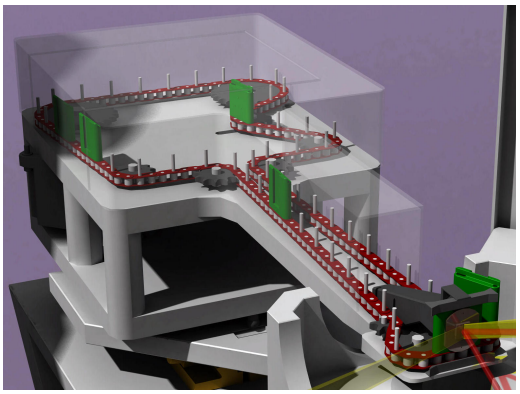

Figure 5.5.: Sample Changer

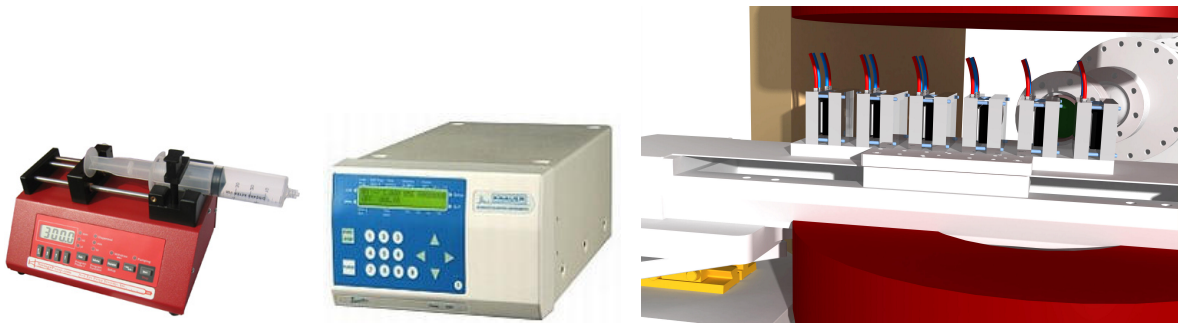

Figure 5.6.: Example of possible items for soft matter experiments (left to right); syringe pump, HPLC pump, sample cells and changer on *Estia*

5.2.5. Soft Matter Sample Environment

Dedicated solid-liquid handling equipment will be build for *Estia* to allow standard soft matter experiments to be performed at the beamline. These will be designed to be compatible with the sample positioning and magnet area to reduce time between changes of equipment and to allow experiments with magnetic contrast variation. It is foreseen that this work package will be done at ESS inside the science support systems group with work payed for from *Estia* construction budget.

Solid-liquid sample cells

A full set of solid-liquid cells similar to the ones already used at other instrument as the D17 reflectometer at ILL will be build. These consist of a silicon block, through which the neutron beam enters and leaves the cell, as well as a liquid holding area with appropriate seal. The cells will include proper mounting options and connections for liquid flow to control the temperature.

Cell changer

To allow quick change between samples, a (linear) sample changer for the solid-liquid cells will be build that fits on the hexapod sample stage with the standard kinematic mounts used for the other sample holder equipment.

Water bath

A commercial standard water bath thermostat will be bought to allow temperature control of the cells between -20°C and 80°C.

HPLC pump

Suitable commercial 4-channel HPLC pump with 0.1-50mL/min will be needed with the necessary mixing capabilities to supply the sample cells.

Syringe pump

For sample injection a multichannel syringe pump with enough connections for all cells on the changer is necessary.

5.3. Non-Sample Environemnt Ancillery Equipment (13.6.9.2.4)

5.3.1. Alginment Laser Assembly

For fast sample alignment and to keep samples in position during temperature changes, a laser measurement assembly will be installed normal to the sample surface as shown in Figure 5.2. The assembly will consist of a diode laser module pointed at the sample surface under $\approx 25^\circ$ to the surface normal and a detection system for the reflected beam consisting of a beam splitter and two cameras with laser line filter to suppress ambient light. The two cameras will be placed at the two output directions from the beam splitter with different distances. By measuring the laser spot positions on the two camera sensors it is possible to extract the sample surface miss-alignment with respect to the ω and χ angles as well as Y-axis position. The feedback from the alignment system will be used to control the hexapod positioning to bring the sample surface into the correct orientation.

5.3.2. Sample Holder Barcodes

The sample holder plates will be engraved with a bar code, that allows unique identification of all holders. When installing a sample in the preparation area, the user will scan this code together with a sample specific code to have unique links between samples and holders. There will be an additional scanner at the sample stage when installing samples into a cryostat and a camera facing the sample position when using the sample changer so the measured sample is always identified.

6. Scattering Characterization System (13.6.9.3)

All neutron optics and characterization after the sample is described within the framework of the scattering characterization system. While in full scope this will also contain polarization analysis equipment, the initial instrument will only contain the neutron detector and flight tube systems.

6.1. Neutron Detector System (13.6.9.3.2)

6.1.1. Detector Arm

Estia will have two detector (one for each vertical beam path) that can be rotated around the sample position on a detector arm at 4 m radius (Fig. 6.1). Initially only one of the detectors will be installed, while the frame will be designed to accommodate both. The detector arm will be a suitable table system, likely built out of aluminum, designed for

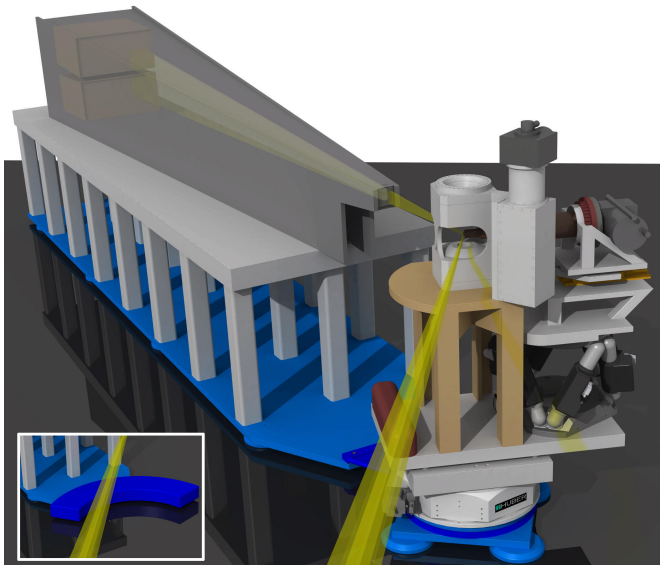

Figure 6.1.: Detector arm with rotation around sample and separate rotation arc (inset)

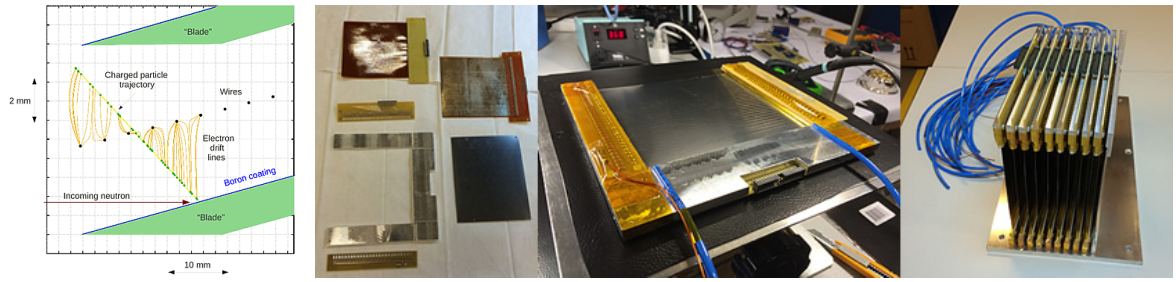

Figure 6.2.: Multi-blade detector concept (left) and components developed by ESS

the attachment for the detectors, analyzer modules and flight tube elements, that will be placed on air feet.

During typical experiments the arm will be attached to the omega base stage of the sample, where the exact detector angle will be measured using an optical encoder. The detector motion will be driven by a wheel attached close to the far end side of the arm.

To accommodate bulky user supplied sample environment the central connection to the rotation center will be removable with an alternative rotation arc to be put into place, that will be mounted on the dace floor with vacuum feet and allow limited rotation without direct connection to the rotation center. This way, the sample stage can completely be removed, opening a space larger than $1\,\mathrm{m}^2$ for SE equipment, for the cost of lower positional accuracy.

6.1.2. Multi-Blade Detectors

Detectors for *Estia* are developed by the ESS detector group based on ^{10}B absorption within a detection gas atmosphere using a concept coined multi-blade. Neutrons hit a thin B_4C coated substrate under a grazing angle (5°) and the charged particle cloud created in the detection gas is measured with a grid of wires, allowing a 2D position sensitivity. Several of these coated "blades" are placed in one detector vessel to achieve a coverage of the full detector size. The advantage of this grazing angle technique is the enhanced detection probability, large saturation count rate per area and increased resolution in on direction (horizontal in case of *Estia*). Detection can be performed with ambient pressure gas, allowing very thin windows to avoid scattering of neutrons at the entrance.

Although these systems are still under active development, it is expected to achive detection efficiencies of ≈60% at 4Å and a resolution of $0.5\text{x}2\,\mathrm{mm}^2$. Two of these detectors with $500\text{x}250\,\mathrm{mm}^2$ detection surface will be installed in the full-scope instrument, allowing the simultaneous detection of specular and off-specular beams from both vertical paths as well as the reflections from the polarization analyzers. The initial instrument will be built with a single detector and analyzer, sufficient for one beam path, but the

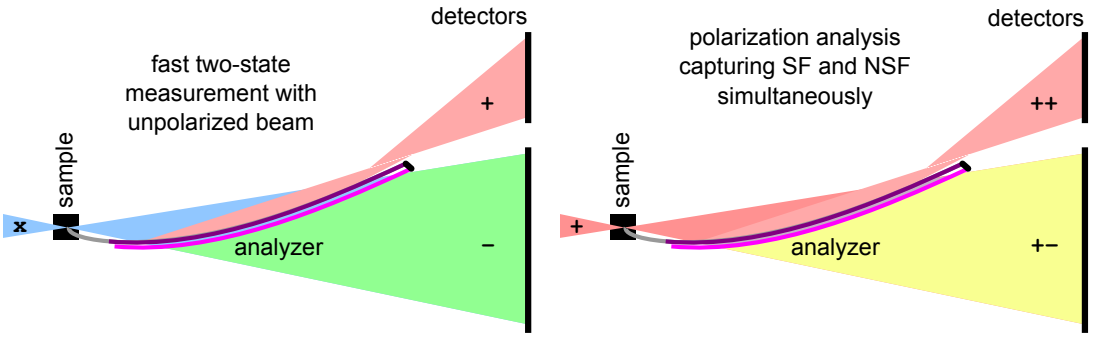

Figure 6.3.: Polarization analysis concept for fast half-polarized measurements (left) or two state polarization analysis (right).

design will be optimized to accomodate two systems without large modifications. Neutron absorbing material will be placed on all sides of the detectors not facing the sample to reduce background from neutrons entering the detector from arbitrary directions.

6.2. Polarization Analyzer System (13.6.9.3.4)

The polarization analyzer for *Estia* uses a similar approach as the polarizers descibed in section 4.5.1. A polarizing supermirror with spiral shape intersects the beam after the sample under constant angle. In contrast to the polarizers a set of two subsequent mirrors is used and the geometry allows to also capture the reflected beam with the detector (Figure 6.3). To achive good polarization for both spin-states, the first mirror is only coated on one side as a reflection polarizer while the second is inclined with a slighly larger angle and double sided coating. The reflection of the second mirror is captured by an absorbing layer at the end of the system.

With this configuration the spin-up state is only reflected once by the first mirror, which leads to good polarization, while the transmitted beam passes through 3 polarizing layers. To adept to the different inclination angles the two systems will have different coatings, m=4 and m=5 are estimated with the current geometry.

6.3. Flight Tube System (13.6.9.3.2.3)

The flight path between sample position and detectors will be filled with Ar gas to reduce intensity loss and background from air scattering. This will be achieved by having a tapered, rectangular flight tube with thin aluminum foil windows installed on the detector arm, filled with a constant flow of Ar gas. The sides of the flight tube and the entrance window geometry will be chosen to allow any beam path from the sample to the detector and avoid reflections from these walls back into the detector.

An additional purpose of the flight tube is the shielding of the detector against neutrons not originating from the sample (e.g. cave walls). Therefore the building material will be neutron absorbing as B-Al or coated with neutron absorber material.

7. Optical Cave (13.6.9.4)

The area within the biological shielding between the first keystone and the experimental cave will be characterized as optical cave. It contains most parts of the second *Selene* guide, the middle focus apertures, polarizers and frame-overlap mirrors.

As can be seen in Figure 7.1, the shielding around the optical cave will mostly be similar to the *Selene* 1 shielding with an additional chicane and entrance door to allow access without opening the shielding elements.

The area will be connected to all utilities and control systems necessary to support the installed equipment including motion control and vacuum systems. PSS equipment for search and access control will be present as necessary.

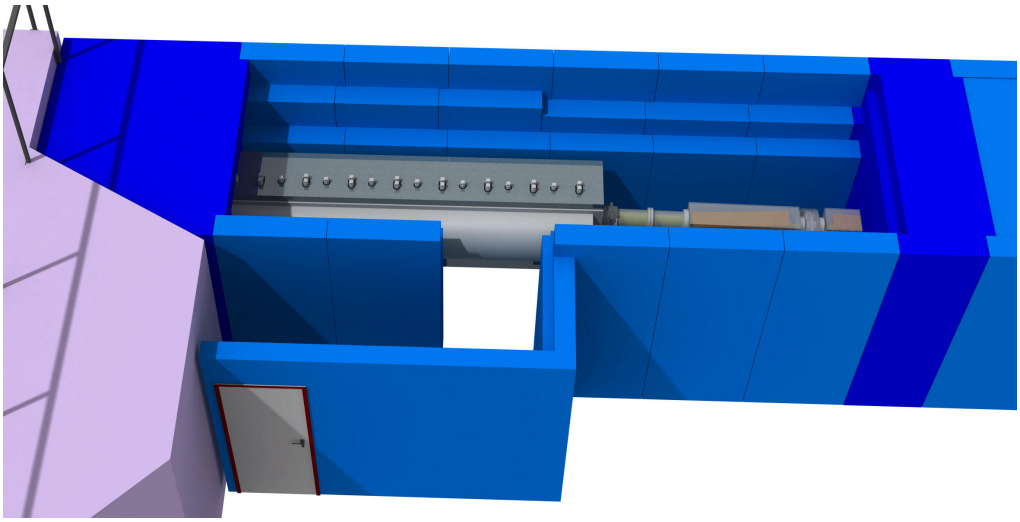

Figure 7.1.: Optical cave area with separate entrance for maintenance access

8. Experimental Cave (13.6.9.5)

At the end of the second *Selene* guide is the experimental cave with the in-cave optics, sample exposure system and scattering characterization system. This is the area commonly being entered by users performing experiments through a PSS controlled door behind a chicane on the down stream side. The whole floor level of the experimental cave will be slightly elevated to achieve a convenient beam height at the sample position. A polished dance floor will be installed covering the whole detector rotation area as well as the sample and in-cave optics table region of the cave.

In addition to all utilities and control systems necessary to support the installed components (motion control, vacuum, gas and cooling water connectors, power) the cave will be equipped with detector electronics and PSS equipment for access control, emergency buttons, fire protection and oxygen level monitoring. A control terminal to access motion control software will be present at one of the cave walls as well as a work bench for sample handling and small maintenance tasks.

To allow independent installation of SE equipment the cave ceiling will have roof access and a 2x2 m^2 access door above the sample area. A local crane will be installed with enough reach to move equipment from in front of the cave entrance to the access door. A camera will be installed to enable remote viewing of the cave while the door is closed.

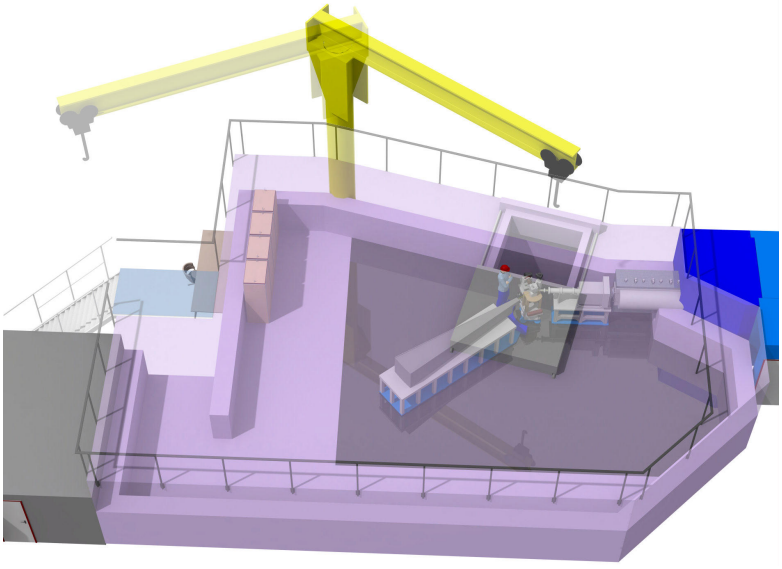

Figure 8.1.: Experimental cave area with optics, sample and detector arm

9. Control Hutch (13.6.9.6) and Sample Preparation Area (13.6.9.7

An instrument control hutch with enough space to allow two user groups working simultaneously will be built downstream of the experimental cave. It will contain the control racks for the equipment installed in the experimental cave build into one wall (avoiding exhaust heat and noise from the equipment to enter the room) and separate control and data analysis terminals.

As with the optical and experimental caves the hutch will be connected to all necessary utilities, control systems, air conditioning and networking.

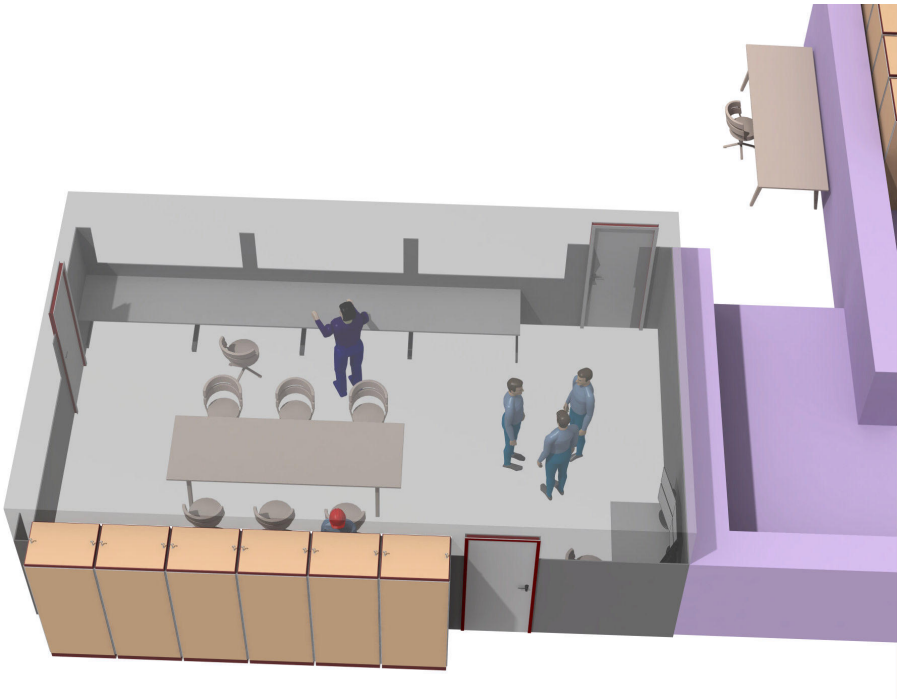

Figure 9.1.: Control hutch and sample preparation area

A dedicated workbench close to the experimental cave entrance will be the sample preparation area.

9.1. Sample Preparation Equipment

To avoid long downtimes all steps necessary to prepare the samples for the experiment will be performed outside the cave in the designated area. This necessitates certain equipment being available at the workbench.

9.1.1. Sample Alignment

To pre-align samples already outside the cave, a special alignment frame will be installed at the workbench. This frame will have a dedicated slot for the sample holder plates and a laser system that will allow to roughly measure the surface height and ω offset. Due to the kinematic mount at the sample stage the installation of the sample will be reproducible. With the height information the users will be able at this stage to adjust the height of the neutron absorbers attached to the sample holder using specialized tools.

9.1.2. Cleaning

The workbench will be equipped with the necessary materials and solvents for standard cleaning of thin film samples. To dry off the surfaces and remove dust a pressurized air pistol with appropriate particle filter will be installed.

9.1.3. SE Stages

Removable SE equipment like the cryostats will have dedicated stages at the preparation area to allow sample installation without danger of damage to the equipment. Necessary connectors for testing of SE equipment (e.g. electric fields) will be installed, as well.

10. Support systems

10.1. Utilities Distribution (13.6.9.8)

AC power lines 230V 50 Hz and 400V 50 Hz will be installed at different positions along the instrument. An EPICS network and a generic Ethernet network should be available inside these areas, too. Artificial Illumination is foreseen inside both caves.

A PA System might be installed inside the cave for communication with the control hutch. A false floor will be evaluated as a possibility to place cable containments and cable trays underneath. This might be done without much additional cost as the floor needs to be elevated already.

A closed chill water circuit will be available for thermal stabilization of components as well as for cooling electronics. A compressed air distribution line will be available in the cave and sample preparation area. Gas lines for Ar and N^2 as well as provisional lines for detectors gas blend will be installed.

10.2. Support Infrastructure (13.6.9.9)

The SE Utilities board distribute media and signal interfaces to auxiliary sample environments that could be installed in the instrument will likely be installed within the experimental cave.

The instrument infrastructure consists of all the conventional construction and utilities (power, cooling water, vacuum, etc.) required to house and operate the technical components.

10.3. Control Racks Hall 1 (13.6.9.10.1)

Control racks will mostly be installed in the wall of the control hutch. Any control equipment where fast access is not necessary can be placed closer to the individual components within the caves or outside the biological shielding. This will mostly be for in-cave equipment for detectors and for motion control of the *Selene* guide adjusters.

10.4. Integrated Control and Monitoring (13.6.9.11)

The software components of the instrument are provided by the DMSC and hence are outside the formal scope of the instrument construction project. Yet the software needed to operate the hardware as well as to process and analyze the scientific data is absolutely necessary for the productive operation of the instrument. A short description of the software is given below.

The software to control the hardware components in order to perform an experiment and for instrument maintenance is clearly integral to the instrument. It is not, however, obvious to what extent the data processing and analysis software should be provided by the ESS and to what extent by the users.

10.4.1. Instrument Control Software

The instrument control software consists of the software components needed to control all the instrument parameters such as motor positions, chopper phase, vacuum system and so on, including graphical user (GUI) and scripting interfaces. The instrument control software serves both the users setting up their experiment and ESS staff for diagnostic and maintenance purposes. The control software interfaces with the Experimental Physics and Industrial Control System (EPICS) framework, which is used to control the individual hardware components.

The instrument control software framework will be standardized across the instrument suite and instrument specific functionalities will be implemented in that framework. The scientifically oriented functions will be scripts that can be called from the GUI as well. The basic functionality requires setting incident wavelength band, chopper speed, VS and slit size, sample orientation (position and incident angle), detector angle as well as sample alignment with the laser system. An important part will be the raw data visualization (detector coordinates, angles and reciprocal space coordinates) and proper normalization by standard measurements. In addition, experimental planning procedures are essential.

10.4.2. Data Processing and Analysis

For data processing the data aggregation, streaming and writing to memory will follow a DMSC standard setup that will be described in detail when the relevant DMSC standard becomes available. Data reduction, normalization and analysis procedures needed for the different operation modes of *Estia* a described in a separate document. The most basic need, however, is to be able to process the raw event data to generate reflectivity datasets as q vs R curves, that can be used by common simulation software.

10.4.3. PSS Integration

In addition to providing safe operation and access to the instrument components, the PSS should allow feedback to the main control software to be able to quickly evaluate conditions that prohibit opening the shutter or leading to alarms. The reverse direction would be necessary for the instrument controls to be able to open the instrument shutter remotely.

11. Selene Guide R&D Project

The custom solutions that are necessary to achieve the desired accuracy for the *Selene* guide mounting and adjustment pose a large risk for the project in terms of finances as well as final performance. For this reason a development project to build a demonstration device will be carried out already during the detailed design phase of *Estia*.

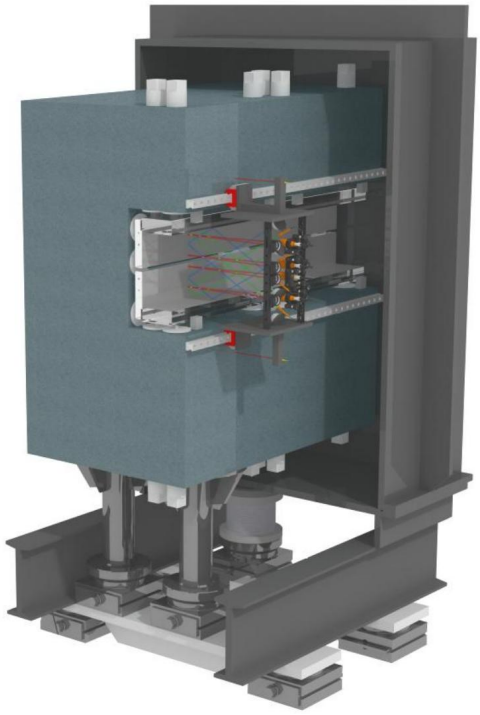

Figure 11.1.: Selene Demonstrator

The demonstrator (Fig. 11.1) will consist of a shorter piece of granite carrier capable of supporting two full sets of mirrors. For cost reasons and to help with the reference measurements the used mirrors will be flat, but with the same heavy backbone and mounting points as the final design. As in the *Estia* system, the granite will be mounted on thermalized, adjustable posts within a vacuum chamber. A shorter version of the metrology cart system will also be available to be able to fully test the adjustment mechanism. In addition to the parts present in the final assembly, the demonstrator will be equipped with vacuum flanges, windows and sensors for e.g. temperature to support the test measurements.

After completion of the demonstrator it will be used to test different adjuster and mounting options for accuracy, repeatability and time stability. Independent measurements of the mirror adjustment will allow the test of the metrology cart system, too. The internal and external sensors will be employed for long term stability tests of the motor control, temperature stabilization and vibration damping capabilities of the system.

The experience gained in the assembly and testing with the R&D project will be used to improve certain aspects of the final design and streamline the installation process of the final product at the ESS site. After the initial tests the demonstrator will be available to be used by the ESS MCA group as well as DMSC for their integration development.

12. Process & Instrument Diagram

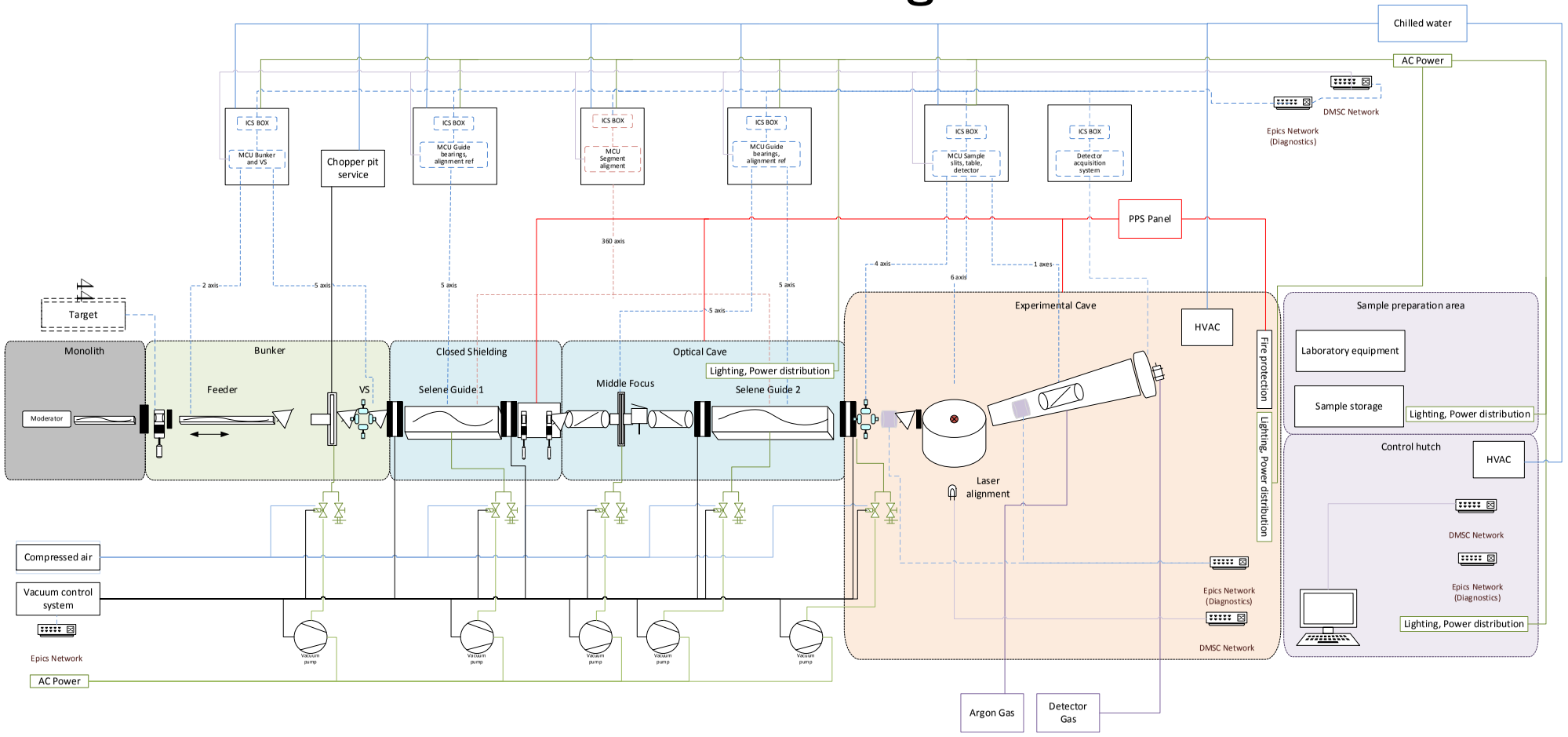

13. Preliminary Safety Analysis

The main hazards present at the instrument are ionizing radiation, liquid gases, oxygen deficiency, fire and moving equipment.

The shielding (4.7) protects personnel outside the instrument from radiation hazards. For changing samples users need to have access to the experimental cave without being exposed to radiation. For maintenance purposes all parts of the instrument also need to be accessible to ESS staff. This is achieved safely with the beam cutoff system (4.7.4). The gamma shutter (PBS 13.6.9.1.8.2) located immediately outside the target monolith stops radiation emanating from the target when the proton beam is not on target and allows maintenance work to be performed on downstream components upstream from the instrument shutter.

PSS access control will prevent opening any of the shielding components in a non-safe state and only allow access to the experimental or optical caves when the instrument shutter is closed and no harmful radiation is measured by the monitoring system. A search procedure ensuring that no people are inside is required to close the interlock and open the shutter. This needs to be performed in either cave if the door has been opened. All interlocked spaces have emergency stop buttons that close the appropriate shutters to prevent radiation exposure. The shutter systems are designed to fail closed.

Oxygen detectors and oxygen level alarms will be installed in the experimental cave if inert gases create an asphyxiation hazard. Fire detection and automatic fire fighting systems will be installed at the instrument.

Operational procedures and safety trainings will ensure safe work with liquid gases as well as other sample environment related hazards. Both caves and the control hutch will have emergency stop buttons to instantly cut off power of any motors accessible within the individual areas.

14. Expected Instrument Performance

Monte Carlo ray tracing simulations with McStas have been performed for the perfect guide geometry of *Estia* using the geometrical parameters used in the preliminary design described in this document. The quantitative results presented in Figure 14.1, although based on a simplified geometry without losses, are directly measurable values that allow evaluation of the transport an imaging properties of the instrument.

To get a feeling for the potential of the instrument during early operations we have performed a virtual experiment using the hight intensity specular mode on *Estia* with just 2 MW of source power. For this virtual experiment a sample of 10x10 mm^2 surface area with a 20 nm film of Nickel on a Silicon substrate is placed at the sample position and measured at 4 different $\theta - 2\theta$ positions. The reflectivity is than calculated from the simulated intensity using a similar data reduction and normalization procedure as will be performed at the beamline. Neutron statistical error is calculated from the counting intensity, but this statistical noise is not added to the data points. The result for short counting times is shown in Figure 14.2.

From these results it is expected, that the goal of measuring 1x1 mm^2 samples is al-

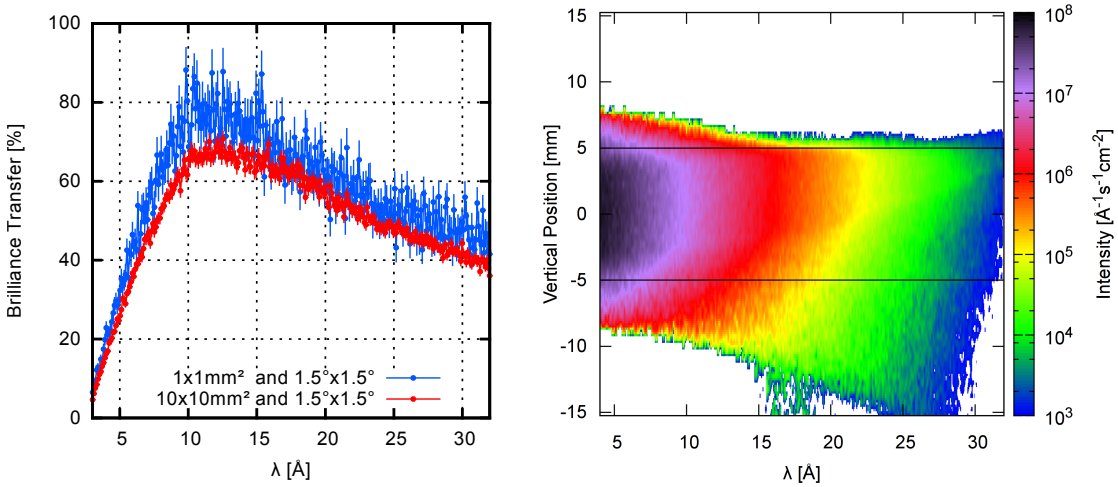

(a) Wavelength dependent brilliance transfer of the guide system for area around the sample.

(b) Wavelength dependent intensity for different hights at the sample position for a 10 mm high virtual source.

Figure 14.1.: Results of McStas simulation.

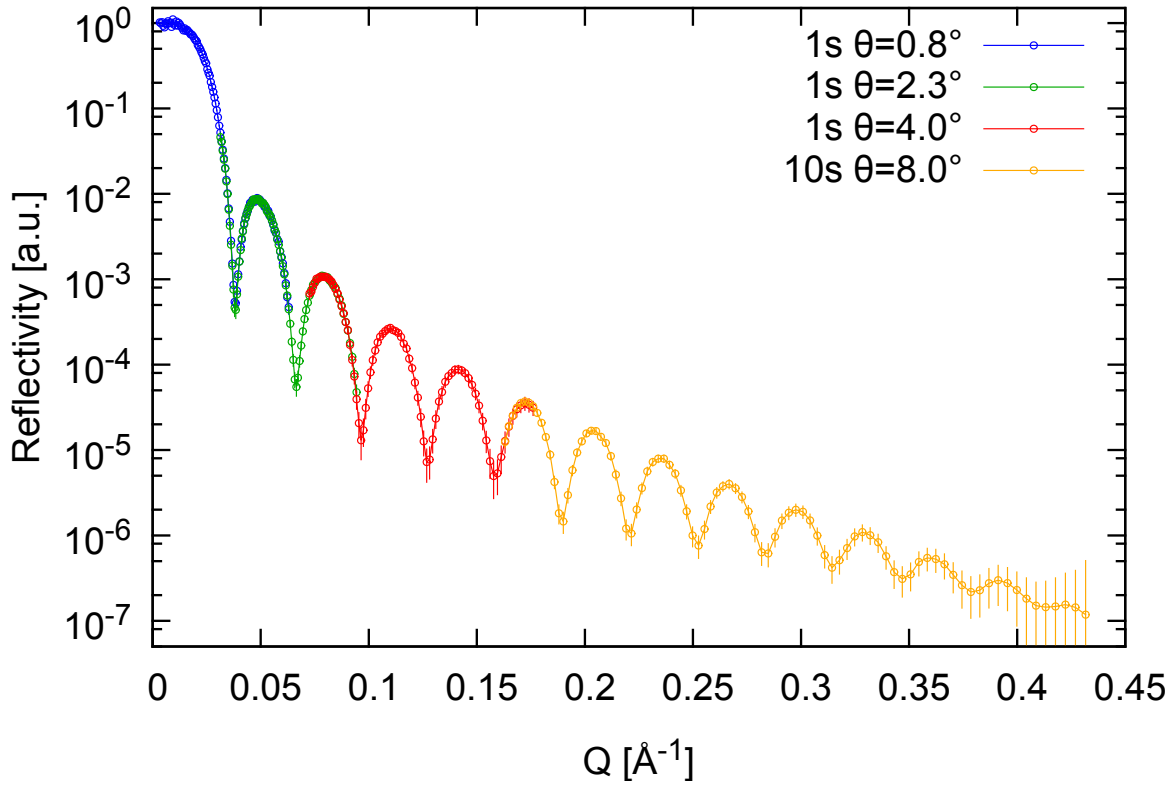

Figure 14.2.: Simulated reflectivity measurement with high intensity mode from 10x10 mm^2 sample of 20 nm Nickel on Silicon.

ready achievable in this early stage of the instrument. The resulting intensity would be approximately 100x smaller, leading to a necessary counting time of just a few hours, a typical experimental time for reflectometry on large samples at reflectometers today. For standard size samples the measurement times are so small, that they are practically only limited by the detector and sample positioning. Time resolved studies would therefore be conducted using 2 pulse skipping mode, giving access to the Q range from 0.001-0.15Å without the need to move the sample.

A. Optics Selection

Estia is designed to allow high quality specular reflectivity measurements on tiny samples down to 1x1 mm^2. To make this possible, the optics need to deliver a large divergence and intensity onto the sample surface while minimizing the amount of unused neutrons that enter the experimental area to achieve outstanding signal to noise ratios. The latter is made possible by the focusing capability of the *Selene* guide, which can project the virtual source onto the sample position. This way, most neutrons that would not get reflected by the sample are already absorbed within the bunker, far away from the experimental cave.

The use of the *Selene* concept already defines the optics between the virtual source and the sample position. With a desired divergence for each of the two beams of 1.5° x 1.5° and 4 Å as minimal wavelength the optimal ellipses parameter and supermirror coating are achieved as described in detail in the *Estia* instrument proposal.

Changes in the ESS source design and dropping of some boundary conditions that restricted the design in the proposal lead to a reconsideration of the feeder concept. The proposed full *Selene* feeder with two elliptical mirrors would lead to an unnecessary long instrument and two additional reflections. A natural choice with the new, high brilliance, butterfly moderator of 3 cm height is a single elliptical guide of the same geometry as the *Selene* guide that follows behind the VS. Although the ellipses has coma aberration, the factor 3 in larger source size still allows a full illumination of the 1 cm high VS.

As the two beam paths need a large, homogeneous divergence profile in vertical direction the two reflections of the elliptical feeder already constitute the optimal divergence profile. Other standard guide concepts would not gather a large enough divergence or lead to an inhomogeneous divergence profile at the VS distance as the minimal distance to the source is 2 m. The main gains of alternative guide solutions would not have considerable impact due to the small source/VS size.

Although the *Selene* guide has 12 m focus to focus distance, the reduction of this distance to 11 m for the feeder to allow a placement of the VS within the neutron bunker did not lead to sizable performance losses in McStas Monte-Carlo simulations. The same holds true for the 600 mm gap between inner and outer feeder that has been compensated by reducing the outer feeder height and extending it's length to still cover the full divergence range. Bringing the ellipsis end closer to the VS increases the coma effects by reducing the apparent beam size for these divergences. While this would reduce the vertical beam size below 10 mm the simulations do not show a reduction in intensity on a 10x10 mm^2 sample within the statistical accuracy of about 5%.

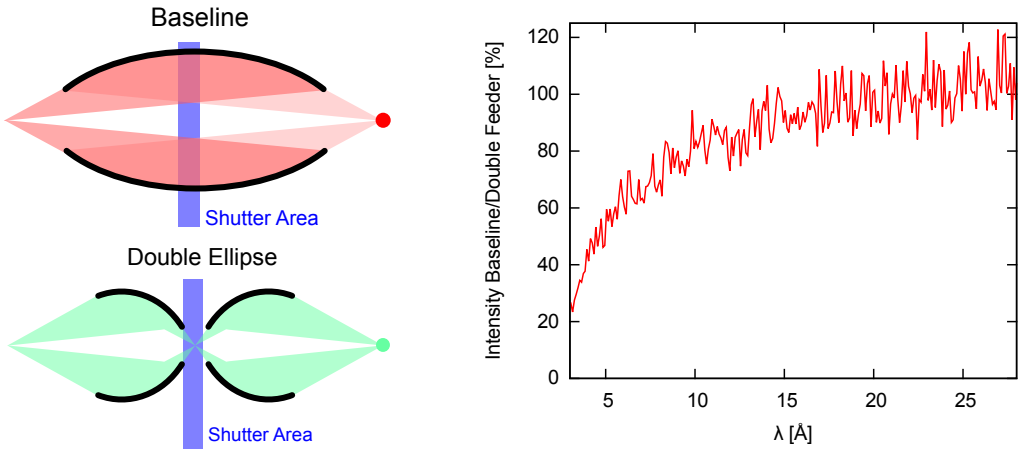

(a) Geometry sketch (b) McStas simulation for 10x10 mm^2 area

Figure A.1.: Feeder geometry baseline and double ellipse compared.

The downside of the elliptical feeder in this geometry is a large opening at the monolith window. Although the *Estia* shielding concept is optimized to reduce high energy neutron background, a second option for the feeder was considered (Fig. A.1a). In this geometry, the single vertical ellipse is replaced by a *Selene* type setup of two elliptical reflectors of 5.5 m focus to focus distance. In contrast to the guide after the VS the geometry was chosen asymmetrically to start at 2.0 m and end at 4.5 m from one focus, which allows the acceptance of the full divergence necessary for the later *Selene* guide. With this geometry the beam size at the monolith window is reduced from 160 mm down to <80 mm, however the increased reflecting angle close to the second focus necessitates a supermirror coating of m=6.5.

Figure A.1b shows the comparison of the brilliance transfer of an elliptical feeder with the latter concept. As can be seen clearly, the long wavelength transport is almost identical to the baseline concept, but the performance drops drastically when reducing the wavelength. The intensity at 4 Å is less than 40% of that of an elliptical feeder, the wavelength where the high q reflectivity with lowest intensity would be measured. Therefore this alternative concept was dropped.

A cost-benefit analysis of initially building two instead of one beampaths has been done for the *Estia* scope-setting meeting. In addition to the increased intensity by a factor of 2, the proposed concept of two beams allows new measurement modes like simultaneous incidence of both spin-polarizations and the ultra small focus option. The main two cost factors for this comparison are the *Selene* guide adjusters and supermirrors. It was decided by the panel, due to external cost constrains, that the ≈1.5 M€ cost increase for building both paths initially outweighs the benefits. This decision was made against the clear recommendation of the instrument team, which estimates an increased cost when upgrading (compared to initially building) the second beam path of more than 1 M€.

Therefore the *Estia* baseline contains a double beam path feeder to make a later upgrade

possible, but only one beam path for the expensive *Selene* guides.

B. Evaluation of H1 and H2 scenarios

This evaluation uses a worst case scenario to evaluate the radiation hazard at a point outside the instrument shielding closest to the radiation source. The results are used to extrapolate the hazard on any point outside the instrument shielding. It is found that even for this event the Estia shielding already fullfills the requirements for normal operation (H1) and thus is sufficient for both scenarios.

Calculation of radiation hazard of an H2 event in Estia:

The event in question is a complete absorption of a fully open beam (maximum beam size passing through the stationary collimation without running chopper) at the sample position by Cd containing material and the subsequent emmission of γ-radiation that needs to be stopped at the experimental cave wall closest to the sample.

- Data for the attenuation coefficient in iron is taken from A. Poskus, Attenuation of Gamma Rays, Vinius University (2012) and extended to higher energies from NIST tables (http://physics.nist.gov/PhysRefData/XrayMassCoef/cover.html).
- Conversion factors for gamma area rate to dose rate uses ICPR-2 table.
- neutron to gamma conversion table from Evaluated Nuclear Structure Data File (ENSDF), which is experimentally validated.

```
In [1]: from scipy.interpolate import interp1d, Rbf

        # load energy dependent attenuation coefficient data for Pb and Fe and
        # generate an interpolator to be able to calculate it for each energy
        data_Fe=loadtxt('/home/glavic_a/Software/ipython/notebooks/gamma_attenuation/Fe_data.png.ext').T
        data_Pb=loadtxt('/home/glavic_a/Software/ipython/notebooks/gamma_attenuation/Pb_data.png.ext').T
        # smooth interpolation, as data is extracted from image and has therefore steps
        mu_Fe=Rbf(data_Fe[0], data_Fe[1], smooth=25, epsilon=0.01)
        mu_Pb=Rbf(data_Pb[0], data_Pb[1], smooth=25, epsilon=0.01)

        # read table of energy dependent conversion coefficients
        # from gamma rate per area to rem/hour: gamma/cm^2 s->rem/hr
        ICPR2_conversion=loadtxt('/home/glavic_a/Software/ipython/notebooks/gamma_attenuation/conversion_factors.dat').T
        gamma_rem=interp1d(ICPR2_conversion[0], ICPR2_conversion[1])

        # read a list of γ-energy vs conversion probablility and select lines above 1% probability and 400 keV energy
        txt=open('/home/glavic_a/Software/ipython/notebooks/gamma_attenuation/Cd_gammas.dat', 'r').readlines()
        Cd_gammas=[]
        for line in txt:
            line=line.strip()
            if line[0]=='#':
                continue
```

```
        try:
            cols=map(float, line.split())
        except ValueError:
            continue
        if len(cols)<3 or cols[2]<1.0 or cols[0]<=400.:
            continue
        Cd_gammas.append((cols[0]/1000., cols[2]/100.))
```

Constants used in the calculations.

```
In [2]: rem2muSv=1e4 # [(μSv/hr)/(rem/hr)]
        wall_distance=1690. # [mm] distance between sample position and closest point outside the cave wall
        n_rate=5e9 # [1/s] rate of neutrons that hit sample area
```

Attenuation factors for Fe and Pb dependant on energy and shielding thickness.

```
In [3]: def atten_Fe(E, d):
            return exp(-mu_Fe(E)*d)
        def atten_Pb(E, d):
            return exp(-mu_Pb(E)*d)
```

Show the accuracy of the smoothed attenuation coefficient for comparison with the mentioned publication.

```
In [4]: E=linspace(0.4, 6.0, 100)

        figure(figsize=(8.0,6.0))
        title('Interpolated attenuation coefficients for iron and lead')
        scatter(data_Fe[0], data_Fe[1], edgecolors='#000066', facecolors='none')
        plot(E, mu_Fe(E), 'b-', lw=2, label='Fe')
        scatter(data_Pb[0], data_Pb[1], edgecolors='#660000', facecolors='none')
        plot(E, mu_Pb(E), 'r-', lw=2, label='Pb')
        xlim(0.35, 6.05)
        xlabel(r'E$_\gamma$ [MeV]')
        ylabel(r'$\mu_{\gamma}$ [cm$^{-1}$]')
        grid()
        legend();
```

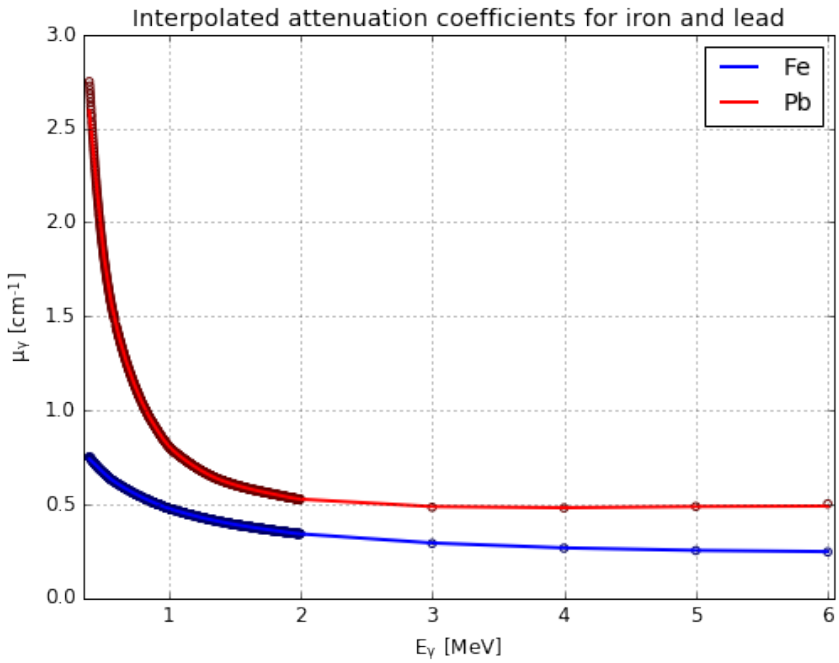

Perform the calculations for Cd absorption over a range of Fe and Pb shielding thicknesses

```
In [5]: dFe=linspace(0., 160., 161)
        dPb=linspace(0., 60., 121)
        DFe, DPb=meshgrid(dFe, dPb)

        A=4.*pi*(wall_distance/10.)**2
        print u'Wall outer distance: %.3f m; sphere area: %.3g cm^2'%(wall_distance/1000., A)

        R=zeros_like(DFe)
        for E, P in Cd_gammas:
            print u'γ(%.2f MeV) yield: %.1e'%(E, P*n_rate), ';   dose rate: %5.2f μSv/h'%(P*n_rate/A*gamma_rem(E)*rem2muSv)
            R+=P*n_rate*atten_Pb(E, DPb/10.)*atten_Fe(E, DFe/10.)*gamma_rem(E)*rem2muSv/A
        print 'Total dose rate: %.3g μSv/h'%(R[0,0])
```

Wall outer distance: 1.690 m; sphere area: 3.59e+05 cm^2

γ **Energy** [MeV]	γ **yield** [1/s]	**dose rate** [μSv/h]	γ **Energy** [MeV]	γ **yield** [1/s]	**dose rate** [μSv/h]
0.56	$5.0{\cdot}10^{9}$	145.45	1.40	$2.3{\cdot}10^{8}$	14.93
0.58	$3.0{\cdot}10^{8}$	9.08	1.49	$1.6{\cdot}10^{8}$	10.82
0.65	$9.5{\cdot}10^{8}$	32.31	1.66	$1.9{\cdot}10^{8}$	13.74
0.65	$9.0{\cdot}10^{7}$	3.07	1.83	$7.4{\cdot}10^{7}$	5.82
0.71	$7.8{\cdot}10^{7}$	2.86	2.10	$6.2{\cdot}10^{7}$	5.45
0.73	$3.0{\cdot}10^{8}$	11.24	2.40	$5.2{\cdot}10^{7}$	4.90
0.75	$8.2{\cdot}10^{7}$	3.14	2.55	$1.0{\cdot}10^{8}$	10.23
0.81	$3.4{\cdot}10^{8}$	14.16	2.66	$1.9{\cdot}10^{8}$	19.02
1.21	$2.8{\cdot}10^{8}$	16.03	2.77	$7.6{\cdot}10^{7}$	8.05
1.28	$1.1{\cdot}10^{8}$	6.83	3.00	$8.0{\cdot}10^{7}$	8.86
1.30	$6.9{\cdot}10^{7}$	4.19	5.43	$7.8{\cdot}10^{7}$	12.73
1.31	$7.6{\cdot}10^{7}$	4.66	5.79	$5.4{\cdot}10^{7}$	9.27
1.36	$3.1{\cdot}10^{8}$	19.68	5.82	$2.0{\cdot}10^{8}$	33.90
1.37	$7.2{\cdot}10^{7}$	4.59	5.93	$5.4{\cdot}10^{7}$	9.34

Total dose rate: 444 μSv/h

Plot the resulting data

```
In [6]: figure(figsize=(8.0,6.0))
        pcolormesh(DFe,DPb,R, norm=LogNorm(1.0, 500.), cmap='gist_ncar')
        colorbar(label='Dose rate [$\mu$Sv/h]', ticks=[1.0, 3.0, 10., 30., 100., 300.]).\
              ax.set_yticklabels(['1', '3', '10', '30', '100', '300'])
        scatter([100],[30], edgecolors='w')
        text(105, 32, u'3 cm Pb\n10 cm Fe\n%.1f µSv/h'%(R[60,100]), color='w')
        contour(DFe, DPb, R, [3.0])
        xlabel('Fe thickness [mm]')
        ylabel('Pd thickness [mm]');
```

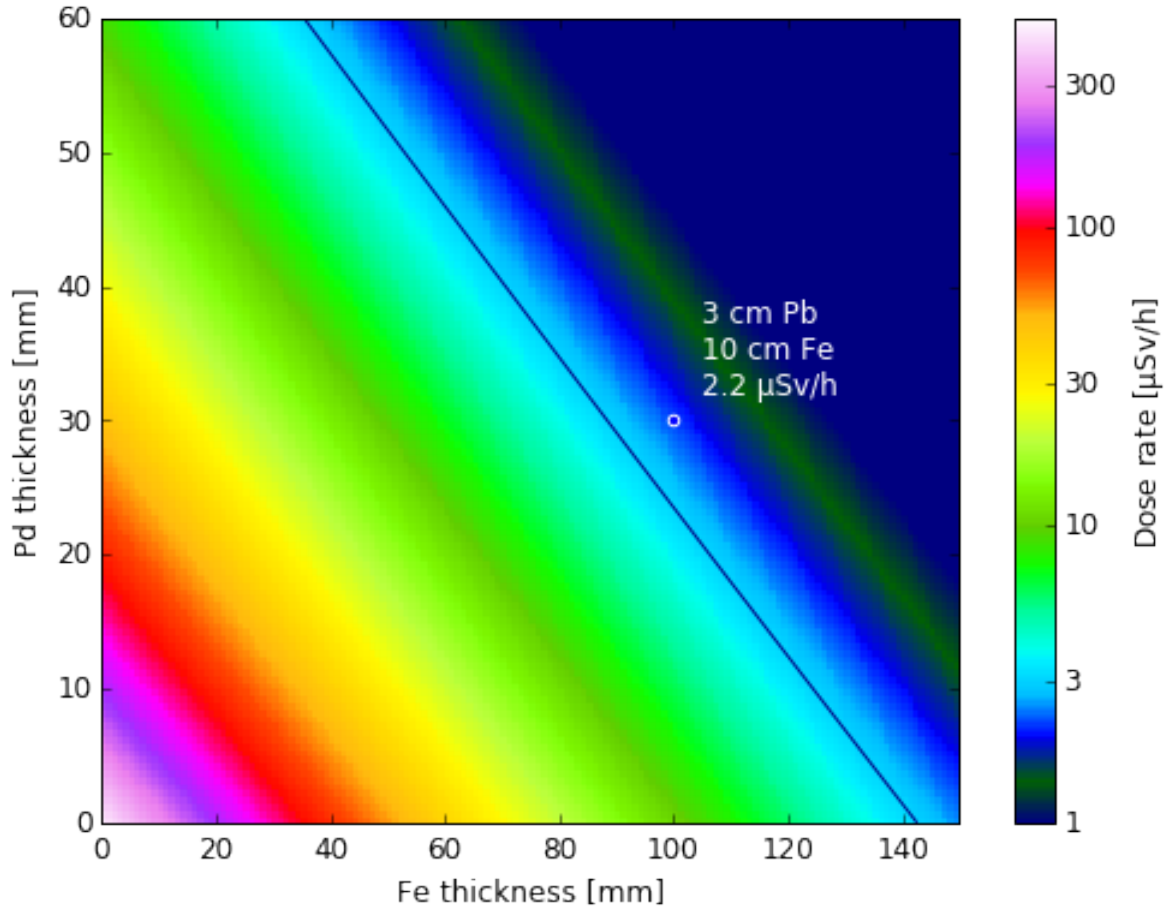

General conclusion for such H2 event:

As can be seen in the plot above, using 5 cm of Fe on the inside and 5 cm on the outside of the proposed wax can cave shielding in conjunction with 3 cm of Pb reduces the produced gamma radiation below a 3 μSv/h threashold. As most of the cave wall is much further away from the sample position then the evaluated

wall it would be enough to add the lead layer on a selected area (2x2 m^2) closest to the sample. All other areas are at least twice as far away, reducing the radiation 4 times so that the pure iron shielding would be sufficient.

As the Estia guide system has only a small loss between the virtual source and the experimental cave and the heavy collimation inside the bunker wall eliminates most fast neutrons, the given scenario is sufficiently similar to evaluate these areas, as well. In the guide section all neutrons will be absorbed by either Boron or Lithium. The Boron absorption produces a softer gamma emission and the steel thickness in that area is 20 cm, therefore the dose rate will be far below the same threashold. Lithium absorption in the shutter has no gamma emission, but produces fast neutrons with an efficiency below 10^{-5}. Although the conversion coefficient from fast neutrons to dose rate is much larger than for gamma radiation, the yield is low enough that the minimal distance to the radiation source alone is sufficient to reach the 3 μSv/h threashold and no further shielding considerations are necessary.

Expansion to normal operation hazard (H1):

As shown above, the Estia shielding reduces the radiation hazard of the complete absorption of all neutrons that could ever reach the experimental cave below a 3 μSv/h level. Any other set of operational parameters (different sample, smaller virtual source) will reduce this by orders of magnitude. This is the given threashold value for normal opetions of ESS instruments and is therefore safely fullfilled with the Estia shielding concept.

Beamstop Considerations:

While the instrument beamstop will be closer to the outer wall of the cave (2-3 times), the absorber to be used is Boron and the wall behind it will contain at least 30 cm of iron shielding material. Although no separate calculation has been carried out, the increase of iron thickness alone will be sufficient to reach a safe level supported by the lower gamma emission energy.

C. Surrounding of *Estia* within the East Sector

The footprint of *Estia* is important to consider in the overall planning of ESS. The two page following this section contain technical drawings of *Estia* placed in the hall geometry. Sketch 1 shows an overview without the beamline shielding together with the instrument $SKADI$ at E3 and a model of the tripple-axis spectrometer $TASP$ at E1 to put the sizes in perspective and show that the neighboring ports at E1 and E3 will still be usable. The second detailed view includes the full beamline shielding and indicates additional information about the minimal possible cave size.

As can be seen there is no overlap with $SKADI$ besides the area directly adjacent to the bunker wall and a small piece of the backside experimental caves of both instruments. In both cases the overlap is similar to the necessary instrument shielding walls which will have to be shared between both instruments. The *Estia* and $SKADI$ instrument teams are in close contact and will work together to coordinate the instrument boundary and look for cost saving opportunities by planning for shared usage of shielding walls. For the usage of port E1 with a monochromator instrument, such as the tripple-axis spectrometer $FLEXX$ currently installed at the BER II facility, the space seems to be sufficient after the access chicane for the *Estia* optical cave is removed. Depending on the installed beamline geometry it would be either necessary to plan this access through the experimental area of that instrument or through the roof of *Estia*.

While the main drivers for the footprint size upstream of the experimental area are the *Selene* guide geometry and the thickness of the necessary shielding walls, the cave structure has to account for several more complex aspects. The position of the sample itself is directly linked to the *Selene* guide focus distances and the direction through which the beam can be extracted in the monolith insert. Depending on the feeder orientation there are only two possible positions, the selected being the one closest to E1. On the E3 side the experimental cave wall (A) needs to be at least 1 m away from the sample position to allow for bulky sample environment. The downstream side of the cave (B) is needed to accommodate the instrument specific crane foundation as well as the beamstop and racks for instrument electronics. In addition, there will be a cable trench beneath the floor that is used to connect the sample environment and instrument components to the hutch outside the cave, which has to be outside the dance floor below the detector arm moving area. The other cave wall distances (C/D) allow the detector arm to move to higher angles, leave space for equipment storage and to be able to pass

by the detector arm when it is positioned at these angles. Some contingency space is include to be able to install additional shielding against background from high energy particles that may be expected from the accelerator tunnel direction (estimated from input by ESS NOS group).

The broken lines on the second sketch mark the smallest possible cave while still keeping the instrument capability. While the cost estimation for the instrument used to establish the costbook value does include the full size cave it may be considered to reduce it at a later stage of the detailed design, if budget pressure demands it. From current estimates the cave structure and shielding cost have been evaluated to 705k€. Reducing it to the dashed size would lead to approximately 42k€ savings.

As described in section 5.2 of the System Requirements document, the necessary detector range for the reflectometry science case is -10° to +80°. While the higher diffraction angles are not within the highest priority core science capabilities of *Estia*, scattering in the backward direction will allow additional broadening of the possible experimental portfolio as well as characterization of the instrument with crystal Bragg-reflections. Removing this capability in addition to the size reduction described above will add additional cost saving opportunities of up to 45k€. Although the backward scattering option might be added with a second detector arm with a smaller sample to detector distance, the additional costs will be of the same order of magnitude as the savings from the instrument cave. This alternative has both benefits and downsides and will be considered during the detailed design phase.

The exact shape of the *Estia* cave will be defined during the detailed engineering and design phase that will begin in 2018/2019. At this time the boundary conditions from ESS side will be more clear and allow the assessment of the necessity to reduce the footprint.

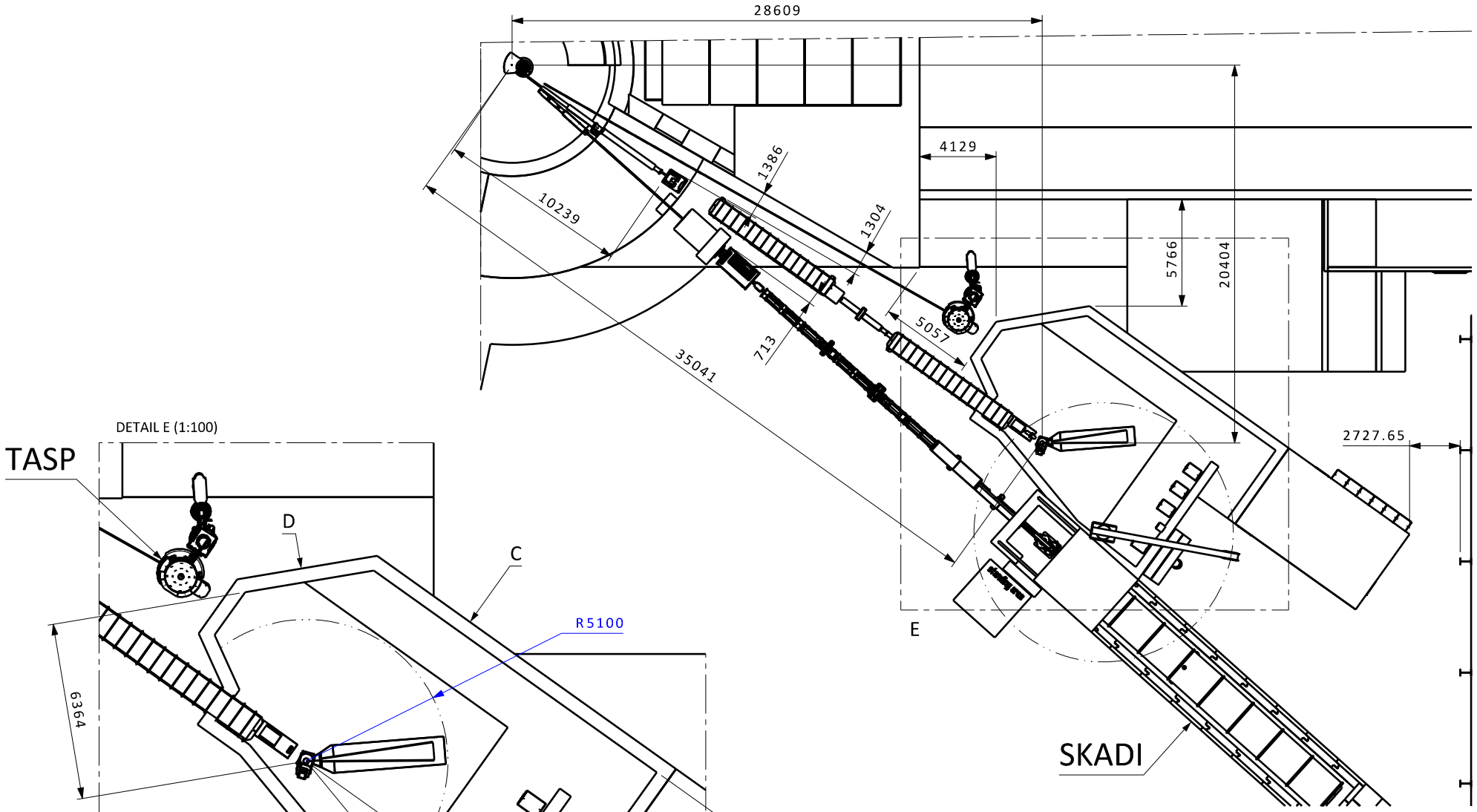

ASSY WEIGHT: - kg	DRAWING TYPE; TITLE; SUPPLEMENTARY TITLE - 13.6.9_ESTIA environment		
General Tolerances			
Linear Dimensions, Form and Position: ISO 2768-mK	MODELED BY: svenschuetz	DATE: 08/12/2016	DRAWING NUMBER: ESS-0087807.2
Chamfers, Radii and Angular Dim's: ISO 2768-vK	DRAWN BY: svenschuetz	DATE: 08/12/2016	LIFECYCLE LABEL: Preliminary; REV.: 1.0; SHEET: 1/2
SURFACE FINISH Min. Ra 3.2	CHECKED BY	DATE	
Documentation protection as per ISO 16016	APPROVED BY	DATE	CAD SOFTWARE: CATIA V6; MC: M4; SIZE: A2; SCALE: 1:150
EUROPEAN SPALLATION SOURCE; DESIGN SITE: ESS Lund	This drawing is produced to ISO 1101, 8015 and 1302		

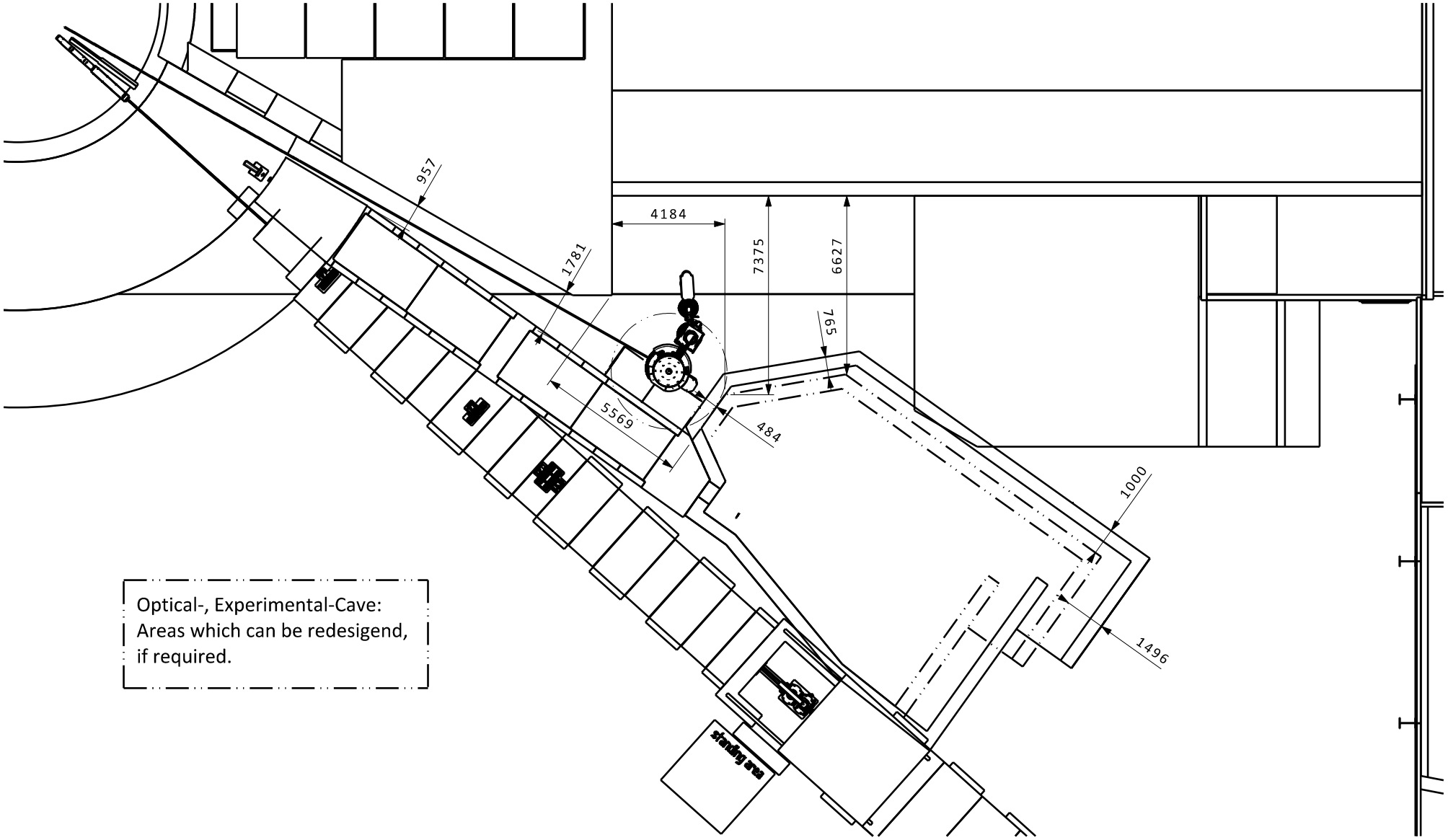

Optical-, Experimental-Cave:
Areas which can be redesigend, if required.

ASSY WEIGHT: - kg		DRAWING TYPE; TITLE; SUPPLEMENTARY TITLE - 13.6.9_ESTIA environment	
General Tolerances			
Linear Dimensions, Form and Position:	ISO 2768-mK		
Chamfers, Radii and Angular Dim's:	ISO 2768-vK		
SURFACE FINISH Min. Ra 3.2			
Documentation protection as per ISO 16016			
EUROPEAN SPALLATION SOURCE	DESIGN SITE: ESS Lund	MODELED BY: svenschuetz — DATE: 08/12/2016 DRAWN BY: svenschuetz — DATE: 08/12/2016 CHECKED BY — DATE APPROVED BY — DATE	DRAWING NUMBER: ESS-0087807.2 LIFECYCLE LABEL: Preliminary — REV.: 1.0 — SHEET: 2/2 CAD SOFTWARE: CATIA V6 — MC: M4 — SIZE: A2 — SCALE: 1:200
This drawing is produced to ISO 1101, 8015 and 1302			

Bibliography

[1] J. Stahn, U. Filges, and T. Panzner. Focusing specular neutron reflectometry for small samples. *Eur. Phys. J. Appl. Phys.*, 58(1):11001, 2012.

[2] J. Stahn and A. Glavic. Focusing neutron reflectometry: Implementation and experience on the tof-reflectometer Amor. *Nuclear Instruments and Methods in Physics Research Section A: Accelerators, Spectrometers, Detectors and Associated Equipment*, 821:44–54, June 2016.

Referenced ESS Documents

ESS-0001786 Definition of Supervised and Controlled Radiation Areas

ESS-0033150

ESS-0034258

ESS-0038078 ESS Sample Environment Mechanical Interfaces for Instruments

ESS-0039408 Handbook for partners to use in design of neutron optics and shielding on instrument beamlines

ESS-0039747

ESS-0041173 Requirements specification for CHIM, Chopper system connection plate intended for use at the ESS

ESS-0041175 Requirements specification for CHIM, Chopper system Umbilical intended for use at the ESS

ESS-0041943

ESS-0042895

ESS-0042906 Requirements specification for Chopper control systems Communications

ESS-0052625 Guidelines for the Design of Radiation Safe Instrument Shielding